

THESIS FOR THE DEGREE OF LICENTIATE OF ENGINEERING

The Enemy Below – Adhesion and Friction of
Ship Hull Fouling

DINIS SOARES REIS DE OLIVEIRA

Department of Mechanics and Maritime Sciences

CHALMERS UNIVERSITY OF TECHNOLOGY

Gothenburg, Sweden 2017

The Enemy Below – Adhesion and Friction of Ship Hull Fouling
DINIS SOARES REIS DE OLIVEIRA

© DINIS SOARES REIS DE OLIVEIRA, 2017.

Technical report no 2017:11

Department of Mechanics and Maritime Sciences
Chalmers University of Technology
SE-412 96 Gothenburg
Sweden
Telephone + 46 (0)31-772 1000

Printed by Chalmers Reproservice
Gothenburg, Sweden 2017

Note on the title

This thesis borrows part of its title from a novel by British Royal Navy officer Denys A. Rayner, *The Enemy Below*¹ [1956], adapted to cinema by Dick Powell in 1957. In the current context, it is meant to symbolize the struggle against marine ship fouling, which has accompanied mankind ever since the first ship set sail to sea.

¹According to worldwide trademark databases, the expression “The Enemy Below” is not currently protected:

- USA Trademark Database:
<https://tmsearch.uspto.gov> [Last accessed: 07/06/2017].
- UK Trademark Database:
<https://trademarks.ipo.gov.uk/ipo-tmtext> [Last accessed: 07/06/2017].
- Swedish Trademark Database (worldwide search):
<https://was.prv.se/VarumarkesDb> [Last accessed: 07/06/2017].

Abstract

Below the waterline, commercial ships are good targets for marine organisms to attach and proliferate, a problem commonly known as *biofouling*. A fouled hull means higher hydrodynamic resistance, which can result in significant fuel penalties. In a fossil-fuel thirsty maritime sector, this means disadvantages in economic, societal and environmental terms. This thesis presents tools for improving current practices related to hull performance management, focusing on the adhesion strength of marine organisms on different coatings (Paper I) and estimation of fouled-hull penalties (Paper II). In Paper I, knowledge gaps that hinder better matching of cleaning forces to adhesion strength of marine organisms are identified, and conclusions are derived from published adhesion strength data. From this adhesion-strength perspective, it is arguably better to invest in combating early stages of fouling, e.g. during idle periods, than using aggressive methods against advanced stages of fouling after an idle period. Regarding estimation of benefits of hull cleaning from a fuel-saving perspective, Paper II demonstrates that the hull form might be an important parameter to consider at low speeds and for less slender vessels. This thesis further applies a rapid calculation method (Granville method) in estimating the hull condition from vessel monitored data (noon reports). The estimated roughness height can be used as an indicator of the hull condition, with the advantage of being independent from vessel speed, which is not the case for other indicators, such as percentage speed loss.

Keywords: biofouling; adhesion strength; in-water hull cleaning; hull grooming; turbulent boundary layer; frictional resistance; roughness; ship resistance; hull form factor.

Acknowledgements

The ongoing project on biofouling is funded by the Swedish Energy Agency (grant agreement 2014-004848). This work would not have been possible without contributions from colleagues involved in the project, supervisors and industry partners. Special thanks to the main project supervisor Lena Granhag (Chalmers), and also to Ann Larsson (Gothenburg University), Rickard Bensow (Chalmers), Kristoffer Tyvik, Patrik Mossberg (Marinvest Shipping AB), Martin Larsson (DFDS Seaways) and Superintendent Lars-Olof Albert (DFDS Seaways). A word of appreciation to Professor Lars Larsson (Chalmers), to Sofia Werner (SSPA) and to Michael Leer-Andersen (SSPA) for interesting discussions. Thanks also to both current and old colleagues, for their support and for making Chalmers a good place to work.

A word of gratitude also to my previous professors and mentors back at Faculty of Engineering of University of Porto, for triggering curiosity and guiding me in acquiring new skills.

Finally, on a more personal note, I would like to dedicate a special word to my family and friends, for being there, beyond borders and idioms.

Appended papers

This thesis is based on the following appended papers:

- (1) Oliveira, D, Granhag, L (2016). Matching forces applied in underwater hull cleaning with adhesion strength of marine organisms. *Journal of Marine Science and Engineering* 4 (4), 66–78.
- (2) Oliveira, D, Larsson, AI and Granhag, L (2017). Effect of ship hull form on fuel penalty from biofouling. Manuscript submitted for publication in *Biofouling*.

The author of this thesis contributed to the ideas presented in the above papers and had a major role in planning, data collection, data processing, preparation and running of experiments, analysis of results and writing.

Contents

List of illustrations	xi
Figures.....	xi
Tables.....	xii
Nomenclature	xiii
1. Introduction	1
1.1. Background.....	2
1.2. Aim and research questions.....	4
1.3. Delimitations	5
1.4. Research ethics, sustainable development and end use of results.....	5
1.5. Thesis outline.....	8
2. Marine fouling and hull maintenance	9
2.1. Marine fouling diversity, recruitment and adhesion	9
2.2. Overview of control methods.....	11
2.2.1. Coating systems.....	12
2.2.2. In-service maintenance	14
2.3. Adhesion strength	15
3. The rough hull penalty	17
3.1. Turbulent boundary layer flow.....	17
3.2. Flow over rough surfaces.....	19
3.3. Previous drag research.....	22

3.4. Full scale roughness effects	23
3.4.1. From lab to ship	24
3.4.2. Monitoring approaches	25
4. Discussion.....	27
4.1. Marine fouling adhesion	27
4.2. Triggers and maintenance assessment.....	29
4.3. Methodology.....	36
4.4. Future work and recommendations	38
5. Conclusions	41
References	43

List of illustrations

Figures

Figure 1 – Overview of main research questions. 4

Figure 2 – Most common types of hull fouling on merchant vessels: a) continuous slime layer (micro); b) interspersed slime (micro); c) filamentous algae (macro); d) encrusting bryozoans (macro); e) tubeworms (macro); f) barnacles (macro). Image sources: a-b) author’s own archive; c-f) courtesy of Marininvest Shipping AB (Gothenburg, Sweden; reproduced with permission). Approximate scales apply to the top right corner of each image..... 10

Figure 3 – Simplified representation of boundary layer flow around the fore body of a ship hull (section at constant depth). Girth-wise direction z is normal to both x and y . The bow is on the left. Only the starboard side of the hull represented. 17

Figure 4 – Arbitrary roughness profile, peak-to-valley roughness height k_t , and the concept of virtual origin, where ε is the wall origin error. 20

Figure 5 – Two examples of roughness functions: Nikuradse’s uniform sand roughness function (Nikuradse 1933) and Colebrook-type roughness function (Johansson 1984). 21

Figure 6 – Alternative iterative procedure for applying the Granville method, where the Granville method calculates resistance penalties (ΔR), given a certain hull roughness condition (k_s), which can be translated into fuel penalties (ΔP) after estimating the propulsive coefficient (η_D). 32

Figure 7 – Speed loss and measured speed through water for a tanker in a period of 3 years. Hull and propeller cleaning events are marked with vertical lines. .. 34

Figure 8 – Evolution of equivalent sand roughness height for a tanker in a period of 3 years. Hull and propeller cleaning events are marked with vertical lines. Estimated equivalent roughness before cleaning (red plus signs) was calculated from divers' reports (Chapter 3, Equation 6), while equivalent roughness after cleaning (green plus signs) were estimated as 100 μm , assuming a deteriorated coating (Schultz 2007). 35

Figure 9 – Increase in resistance ΔR [%] relative to a hydraulically smooth hull (circles), and idle time (green line), for a tanker in a period of 3 years. Hull and propeller cleaning events are marked with vertical lines. Reference speed and draft correspond to 14 kn and 12.2 m, respectively. 36

Tables

Table 1 – Main vessel specifications for a tanker. 34

Nomenclature

B	ship's breadth [m]
C_B	block coefficient, $C_B = \nabla / (L_{WL} B T)$ [-]
C_f	local skin friction coefficient, $C_f = \tau_w / (\frac{1}{2} \rho U_\infty^2)$ [-]
C_T	total resistance coefficient, $C_T = R_T / (\frac{1}{2} \rho U_\infty^2 S)$ [-]
ΔC_f	change in local skin friction coefficient, $\Delta C_f = C_{f,rough} - C_{f,smooth}$ [-]
ΔC_T	change in total resistance coefficient, $\Delta C_T = C_{T,rough} - C_{T,smooth}$ [-]
Fr_S	ship's Froude number, $Fr_S = U_{STW} / \sqrt{gL_{WL}}$ [-]
k_s	equivalent uniform sand roughness height [m]
k_t	peak-to-valley roughness height measured within a linear length of 50 mm [m]
K	form factor (ITTC-78) [-]
g	gravitational acceleration [m/s ²]
L_x	longitudinal distance from the bow [m]
L_{WL}	waterline length [m]
P	shaft power, $P = R_T U_{STW} / \eta_D$ [W]
ΔP	change in propulsive power due to hull roughness [W]
R_T	total towing resistance [N]
ΔR	change in resistance due to hull roughness [N]
Re_S	ship's Reynolds number, $Re_S = L_{WL} U_{STW} / \nu$ [-]
Re_x	Reynolds number based on longitudinal distance from the bow and vessel speed through water, $Re_x = L_x U_{STW} / \nu$ [-]
S	wetted surface area [m ²]
T	ship's draft [m]

t	time [s]
U_{STW}	ship speed through water [m/s]
U_{SOG}	ship speed over ground [m/s]
U_δ	time-averaged velocity magnitude at boundary layer edge [m/s]
U_∞	free-stream speed [m/s]
u, v, w	time-averaged velocity components [m/s], corresponding to each of direction x, y, z
u_τ	wall shear velocity, $u_\tau = \sqrt{\tau_w/\rho}$ [m/s]
x, y, z	longitudinal tangential, normal and girth-wise tangential coordinates on the hull [m]
Π	wake parameter [-]
δ	boundary layer thickness [m]
∇	volume displacement [m ³]
ε	wall origin error [m]
κ	von Kármán constant [-]
η_D	propulsive coefficient [-]
ρ	density of the fluid [kg/m ³]
ν	kinematic viscosity of the fluid [m ² /s]
τ_w	wall shear stress [N/m ² = Pa]

Superscript

+ inner-scaling of a variable, using u_τ for velocity scale, or ν/u_τ for length scale

Subscript

crit critical

m maximum

S ship

Abbreviations

AF	Anti-Fouling paint (containing biocides)
CDP	Controlled-Depletion Polymers
CFD	Computational Fluid Dynamics
EPS	Extracellular Polymeric Substances
FR	Foul-Release coating (non-toxic paint) or Fouling Rating, if followed by hyphen and a number: e.g. FR-40
GHG	Greenhouse Gas
IMO	International Maritime Organization
NIS	Non-native Invasive Species
RoRo	Roll-on/roll-off cargo ship
ROV	Remotely Operated Vehicle
SPC	Self-Polishing Copolymers
TBT	Tributyltin

1. Introduction

He immediately observed the bottom of the boat to be covered with a species of small clam, which, upon being tasted, proved a most delicious and agreeable food.

Owen Chase

Since early ages, it has been recognized that marine life growing on ships' wetted surfaces makes it more difficult to gain speed. Already in the first century A.D., Plutarch identified marine growth as a deleterious factor for performance, and clarified the need for protecting the ship (Plutarch n.d.). Owen Chase, in the above quote from an 1820's shipwreck survival account², only partially recognizes the importance of a clean hull; otherwise, he might also have praised a temporary improvement in hull hydrodynamic performance as a possible factor in his survival.

Today, in spite of a significant advance in technical solutions and knowledge on biofouling mechanisms, hull fouling remains a chronic malady for the shipping industry. This is certainly aggravated by the current fleet overcapacity, which has led to increased idle periods (BRS 2017) that favour the proliferation of marine growth on the hull. In order to avoid idling and also lower the fuel consumption, some shipping segments have also turned to slow steaming (UNCTAD 2016), which however increases the percentage of energy dedicated to overcoming the fouling penalty (Woods Hole Oceanographic Institute 1952). Still, in the current context of low energy prices³, noisy voyage performance data, schedule constraints, uncertainties in fuel consumption measurements and misplaced incentives for improving energy efficiency (Johnson & Andersson 2014), the investment in improving biofouling management might not be at the top of many ship owners' priorities. Nevertheless, the situation will hopefully be improved by recent developments in terms of increased transparency and clearer responsibilities, namely through standard hull performance monitoring methods

² The whale-ship *Essex* sank in 1820 and later provided inspiration for Melville's novel *Moby-Dick, Or the Whale* [1851].

³ In the last decade, crude price reached an absolute low in early 2016, which was more than 4 times lower than the peak value in 2008 (Nasdaq 2017).

(ISO 2016) and special clauses dedicated to hull cleaning in chartering contracts (BIMCO 2013). Additionally, in the wake of the International Convention for the Control and Management of Ships' Ballast Water and Sediments, aiming at preventing the spread of Non-native Invasive Species (NIS), the International Maritime Organization (IMO) has released guidelines for management of biofouling (IMO 2011a). Although such guidelines are currently voluntary, ship owners should be prepared for eventual future developments in similarity to ballast water management.

The “true” cost of hull fouling involves more than direct costs related to speed, fuel and hull maintenance. By increasing required propulsive power, biofouling has an impact on emissions to air from shipping, including greenhouse gas emissions (GHG: CO₂) and air pollutants (NO_x, SO_x and particulate matter). It is estimated that 9-12% of emissions from shipping are due to hull and propeller under-performance (IMO 2011b). In the period 2007-2012, shipping emitted roughly 1 billion tonnes of CO₂ per year (IMO 2014). Although shipping emissions correspond to only ~3% of global emissions, it is argued that shipping should be part of the effort to curb global warming (Anderson & Bows 2012). Additionally, other environmental and societal consequences of a fouled hull must also be assessed, including risks associated with measures against fouling, such as chemical contamination through release of toxic substances from hull paints (Thomas & Brooks 2010) and biological contamination through the spread of NIS (Drake & Lodge 2007). All such consequences are ultimately bound to affect future conditions for life on Earth.

1.1. Background

As soon as a solid surface is exposed at sea, it provides a substrate for some marine species to adhere to and develop during their sedentary life stages. This occurs on both natural and manmade structures, which can be stationary – e.g. buoys and offshore structures – or moving – e.g. ships and recreational boats. Most of the fouling occurs under stationary/static conditions (Dürr & Thomason 2009a).

The submerged area available for biofouling settlement on a single vessel varies widely within the world's commercial fleet, ranging from a couple hundreds of square meters for small-sized vessels, to a few hectares for large-sized vessels (Moser et al. 2016). The development of biofouling communities on ship hulls is determined by a large number of variables (Woods Hole Oceanographic Institute

1952; Dürr & Thomason 2009a). Operational parameters that determine the amount and distribution of fouling on a ship hull include vessel speed, total idle time, dry-dock interval, trade route, port calls (“clean ports” versus “foul ports”), geographical location, distance from shore, temporary permanence in freshwater courses, adequacy of fouling-control system to operational profile of the vessel, integrity of fouling-control system and, finally, the frequency of in-water maintenance (Woods Hole Oceanographic Institute 1952; Brock et al. 1999; IMO 2011a). Numerous environmental variables further complicate the prediction of biofouling development on a ship: local- and season-dependent biofouling pressure (i.e. concentration of propagules in seawater), weather conditions, seawater temperature, salinity, currents, etc. (Wood et al. 2000; Briand et al. 2017). Finally, the design of a ship hull determines the percentage of wetted surface that is sheltered from high hydrodynamic stress (IMO 2011a). These sheltered areas, together with dry-docking support strips (areas not protected by recently applied anti-fouling paint), represent *niche areas*, which usually host a higher degree of fouling and higher diversity of fouling species (Davidson et al. 2009).

Ever since seafarers became aware of issues associated with biofouling, the struggle for an intact and smooth underwater hull has resulted in an overwhelming amount of solutions throughout the history of shipping, most of them with doubtful results in terms of deterring growth (Woods Hole Oceanographic Institute 1952). On wooden hulls, the main target were shipworms, organisms that carve into wood and affect structural integrity. Protection could be achieved by wood treatment or sheathing with various possible materials. Centuries after early usage of copper by Phoenicians, copper was rediscovered around the 17th-18th centuries for its antifouling properties, which were only proven in the 19th century. Meanwhile, with the introduction of iron/steel hulls, copper sheathing was found to be unsuitable, due to accelerated corrosion, so the focus shifted to paint systems, which today still largely rely on controlled release of biocides to seawater (Woods Hole Oceanographic Institute 1952; Yebra et al. 2004). Recent developments in fouling control will be further explored in Section 2.2.

Today, commercial ships usually undergo compulsory dry-docking and hull surveys for safety and structural integrity, as required by Classification Societies, in intervals of roughly 5 years (Takata et al. 2006). Due to associated high costs, dry-dockings are also the only chances for removing damaged paint and repainting the hull, where quick touch-up of damaged areas is normally preferred to an entire hull blasting. Within dry-docking intervals, in-water hull cleaning is a

common practice, especially for vessels operating in tropical zones. Such cleaning events are typically triggered by performance monitoring from voyage data (Munk et al. 2009) or underwater surveys (NSTM 2006; BIMCO 2013). In-water cleaning should be performed in such way as to not damage the existing fouling control paint (IMO 2011a; BIMCO 2013), otherwise risking penalties from increased mechanical roughness (paint roughness and corrosion), as well as a higher biofouling growth rate in the subsequent time period (Malone 1980; Munk et al. 2009).

1.2. Aim and research questions

Hull maintenance comes with a dilemma: on the one hand, economic and environmental reasons call for lowering the amount of fouling on ship hulls (hull performance, fuel consumption, emissions to air and transport of non-indigenous species); on the other hand, control of biofouling comes with other consequences, such as emission of toxic compounds to water (Thomas & Brooks 2010) and release of NIS (Morrisey et al. 2013). The aim of the current on-going project is to explore tools for a compromise between these two sets of impacts.

Main research questions addressed in this thesis are presented in Figure 1 and deal with minimizing underwater hull cleaning forces (appended Paper I) and better estimating performance gains from hull cleaning (appended Paper II). Specific questions dealing with hull cleaning (Paper I) include: discuss the representativeness of laboratory measurements of adhesion strength relative to naturally occurring communities on today's ships; identify the knowledge gaps for optimizing hull cleaning technology. Regarding the fouled hull penalty (Paper II),

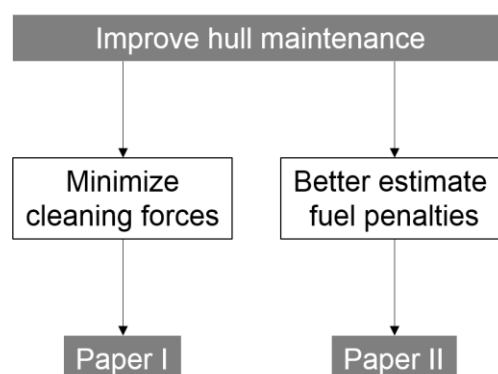


Figure 1 – Overview of main research questions.

cost-effective methods for estimating hull roughness penalties are discussed, revisited and extended.

1.3. Delimitations

This thesis is part of an on-going project that will culminate in guidelines for hull cleaning in the North Sea region. Firstly, the regional focus should be highlighted, since biofouling communities and fouling pressure vary widely across the globe. Nevertheless, conclusions for cosmopolitan species, such as the macroalga *Ulva* sp., should be more widely applicable, although local variations should be acknowledged, such as seasonality, temperature, salinity, etc. Secondly, the present work focuses on forces necessary to remove different degrees of fouling from hull coatings, whereas the design of specific hull cleaning devices is not considered, except in what deals with actual forces applied at surface level, i.e. pressure and wall shear stress.

In terms of hull performance estimation, the propeller roughness condition is not addressed directly. Finally, a full techno-economic assessment of hull maintenance practices, as attempted by Malone (1980), is out of the scope of the current study: even though it is considered as an ultimate goal, such type of assessment must be made on a case-by-case basis and will be dependent on volatile conditions of global trade and shipping economics (Stopford 2009).

1.4. Research ethics, sustainable development and end use of results

This sub-section is dedicated to identifying and analysing important ethical questions concerning this work and, also, potential consequences of the project in terms sustainable development.

The first question regarding research ethics deals with sources of funding. In the current study, funding is provided by the Swedish Energy Agency, which is a state-owned agency, funded by taxpayers. This ensures that no commercial interests are involved. All publications will be made available to the public via Open Access (free downloading from publisher or from an open repository).

In this project, vessel details and performance data are shared between researcher and collaborating shipping companies. This entails that confidentiality must be kept regarding commercially sensitive information, such as routes and

historical data of vessels (location, speed and other details). However, for the current research aim, results can be made publicly available and discussed without referring to an absolute time frame or location of the vessel. Still, any information disclosure is subject to approval from the shipping company, with no damage to the relevant findings of the study.

The project is further analysed in terms of potential benefits and drawbacks of the outcome for several stakeholders (shipping companies, etc.), as well as for the five capitals defined by Stacey & Stacey (2012).

Shipping companies collaborating in the study (ship owners and operators) might gain a better insight on the performance of their vessels, or check their own performance indicators. Also, increased knowledge on hull cleaning forces and consequences of hull cleaning would be a clear advantage. Some sampling procedures might cause temporary, localized damage to the top coating of the hull, which should have minor consequences in vessel performance and will not affect integrity (e.g. deployment of magnetic panels as in Coutts et al. 2007).

The shipping industry, as a whole, might benefit from the outcome, firstly via transparency regarding experimental and numerical methods used in this study (all details are publicly available) and, secondly, via possible implementation of improved practices in the industry: reduced fuel consumption and reduced dry-docking costs related to the underwater hull paint system. Other means of transportation (air- and land-based) might suffer in terms of competitiveness, but this also comes with environmental advantages, as detailed below in this section.

Hull cleaning companies, namely technology developers and users (diving companies), might benefit from clearer standards in terms of forces applied during in-water hull cleaning. Shipyards would also benefit, in the long run, from lower costs concerning environmental protection, assuming reduced need for dry-dock maintenance of the underwater hull. The latter would also result in a lower turnaround time for docking vessels, which would increase business opportunities for shipyards, as current issues with availability of dry docks are well known to the industry (Takata et al. 2006). Paint manufacturers would also benefit, by increasing the success rate of their products and demonstrating performance gains with higher transparency, an aim also preconized by the developers of the ISO 19030 hull performance standard (ISO 2016). However, a hazard exists here for paint companies, in that volume sales could drop as hull cleaning practices and technology improve. However, a likely increase in global seaborne trade (UNCTAD 2016) might more than compensate for this.

The five capitals defined by Stacey & Stacey (2012) correspond to Natural, Human, Social, Manufactured and Financial capitals.

The Natural capital would benefit from reduced GHG emissions, as the shipping industry would reduce its share of emissions through better hull performance. An hazard must be highlighted here, which relates to misuse of the outcome and occurrence of rebound effects (Freire-González & Puig-Ventosa 2015): an improvement in terms of efficient use of a resource ultimately results in increased exploitation of that resource (Jevon's paradox). Although it is likely that, in the case of seaborne trade, an increase in global trade will probably more than compensate for any increase in hull performance, there is no relation of causality here. The rebound effect would instead reside in the individual operational choice, once a clean hull is provided, between keeping a constant power while steaming at a higher speed with a clean hull (as-fouled power), or steaming at lower power while keeping a constant speed (as-fouled speed). However, it is more likely that the second option be chosen (as-fouled speed), at least in the current paradigm of slow steaming (UNCTAD 2016), although a future increase in global trade could also change this. Finally, misuse of the outcome might lead to the spread of NIS, with possible consequences to local ecosystems. Again, guidelines for in-water hull cleaning should aim at minimizing the risk of spread of NIS.

The Human capital would benefit from increased air quality (lower emissions to air), resulting in a positive impact on human health, as ~60,000 deaths per annum are estimated worldwide due to particle emissions from shipping (Corbett et al. 2007). Still, the above remarks concerning rebound effects apply here too. Additionally, care should be taken concerning NIS, as well as diseases and parasites potentially transferred via ship hull fouling (Champ 2000; Swain & Shinjo 2014), which can be released during in-water hull maintenance.

The Social capital should be safeguarded in terms of working conditions for divers, which still perform a large part of the hull cleaning work. Use of remotely-operated vehicles (ROV) for commercial in-water hull cleaning is expanding, as reviewed recently by Morrissey & Woods (2015), which means an increase in both Manufactured capital and Social capital, leading to increased occupational safety in diving companies.

Benefits for Financial capital should be apparent by now to the reader, as cargo and passengers can be transported at a lower cost. Also, the project ultimately provides tools that, in principle, enable setting clearer responsibilities between involved stakeholders (BIMCO 2013; Rehmatulla & Smith 2015). These

tools can potentially be used for improving overall financial performance. Finally, in order to safeguard local economies that strongly depend on the Natural capital, such as tourism, aquaculture, fisheries etc., issues related to the spread of NIS should be safeguarded against, through clear guidelines for hull cleaning.

1.5. Thesis outline

This thesis addresses the main findings of two appended papers, as well as the methodology leading to these findings. Paper I is a review article on adhesion strength of marine organisms, based on a collection of values of adhesion strength published in peer-reviewed literature. Paper II puts forward a hypothesis for improving existing methods used in estimation of the penalty associated with a fouled hull.

Chapter 2 introduces Paper I, giving a description of marine fouling and adhesion mechanisms, together with control methods currently in use.

Chapter 3 introduces Paper II, discussing the theory behind drag penalties due to a rough hull.

In Chapter 4, main findings from each of the appended papers are discussed, together with methodology and an outlook on future research.

Chapter 5 summarizes main achievements.

2. Marine fouling and hull maintenance

What is the composition of ship hull fouling? What are its most common recruitment and adhesion mechanisms? Which methods are available for controlling ship fouling? These are some of the questions addressed in this chapter, as an introduction to Paper I.

2.1. Marine fouling diversity, recruitment and adhesion

Marine organisms found on ship hulls can be grouped into *microfouling* and *macrofouling*, depending on the size of individual organisms or colonies, and also taking into account their stage of development (Dürr & Thomason 2009b). Biofouling can also be differentiated between soft and hard fouling, according to the absence or presence of a calcareous structure, respectively (NSTM 2006). Examples of most common biofoulers on ship hulls are shown in Figure 2, ranging from micro- to macrofoulers, and from soft to hard fouling.

Biofilms, also referred to as marine slimes, are composed of marine bacteria and microalgae (Figure 2a,b). These slimes may also include developing stages of algae and animal larvae, which still classify as microfouling, due to their sub-millimetre scale, even though such forms eventually grow into macrofouling (Figure 2c-f). Individual cells reach a surface mostly through action of currents and gravity, but also, in the case of motile bacteria and spores/larvae, through actively selecting a location for attachment (Railkin 2004). Biofilms are composed of cells, which adhere to the substrate by producing Extracellular Polymeric Substances (EPS) mostly composed of carbohydrates and proteins (Chiovitti et al. 2006; Pettitt et al. 2004). Slimes can also capture a variable amount of silt, i.e. inorganic debris (ASTM D4939–89 2003). Slimes are typically removable by touch, as shown in Figure 2a, but tenacious biofilms have also been reported on ship coatings, against which some of the current more-gentle cleaning methods are ineffective and can even inadvertently select for (Hearin et al. 2016).

Propagules of macrofoulers consist in sub-millimetre spores and larvae that exist in planktonic form, i.e. suspended in seawater. Spores of the macroalga

SOFT FOULING

— 15 mm



a)

— 10 mm



b)

— 50 mm



c)

HARD FOULING

— 25 mm



d)

— 10 mm



e)

— 30 mm



f)

Figure 2 – Most common types of hull fouling on merchant vessels: a) continuous slime layer (micro); b) interspersed slime (micro); c) filamentous algae (macro); d) encrusting bryozoans (macro); e) tubeworms (macro); f) barnacles (macro). Image sources: a-b) author's own archive; c-f) courtesy of Marininvest Shipping AB (Gothenburg, Sweden; reproduced with permission). Approximate scales apply to the top right corner of each image.

Ulva sp. (adult form in Figure 2c) are initially motile, using their flagella to actively select a substrate according to environmental and surface cues. Once the right conditions are met, algal spores adhere irreversibly by secreting an adhesive glue (Callow & Callow 2006).

Barnacle larvae, which later develop into hard macrofoulers (Figure 2f), are capable of exploring the surface to which they eventually attach (Larsson et al. 2016). A chemically different adhesive from that used for settlement mediates temporary adhesion, as the barnacle “walks” over the substrate. Finally, the barnacle metamorphoses into its adult stage, producing a stronger cement for permanent adhesion to the substrate (Crisp et al. 1985; Kamino 2006).

Other types of macrofoulers rely on substantially different recruitment and adhesion mechanisms. Encrusting bryozoans (Figure 2d) can propagate from a single attached individual, growing into a colony (Woods Hole Oceanographic Institute 1952, pp.77–78). Tubeworms (Figure 2e) adhere to the substrate by secreting a simple adhesive that holds together a tube wall, which contains the fully mobile individual (Sagert et al. 2006).

On extremely fouled vessels, mussels will also recruit at some point (not shown in Figure 2). These bivalves attach to the substrate using a specialized holdfast, the mussel byssus, which consists in a group of threads, each equipped with an adhesive plaque. The individual mussel can then control the tension of the threads, and even move to a new location by breaking threads and growing new ones (Crisp et al. 1985; Sagert et al. 2006).

2.2. Overview of control methods

Prevention of fouling has been a topic for at least 2,000 years⁴. Today, fouling control requires two types of intervention: dry-docking of vessels, and in-service maintenance.

During dry-docking, the underwater paint system is repaired. In the worst case this means complete blasting of the hull for removal of old layers of paint and corrosion, followed by application of a complete paint system, including anti-corrosive primers and layers of fouling-control paint (Townsin et al. 1980). In-

⁴ For a thorough historical perspective on prevention of fouling, please refer to Woods Hole Oceanographic Institute (1952) and Yebra et al. (2004).

service maintenance includes occasional in-water cleaning for removal of growth, usually performed together with propeller polishing (Malone 1980).

2.2.1. Coating systems

The paint system for the underwater part of the hull serves two purposes: minimize corrosion through an epoxy barrier coat applied directly onto the steel plating, and minimize drag through top coatings that prevent biofouling and result in a surface as smooth as technical/economically possible (Townsin et al. 1980).

Commercial topcoats for fouling control fall into two broader categories: Anti-Fouling paints (AF) and Foul-Release (FR) coatings. AF paints rely on the controlled release of compounds that inhibit growth, i.e. biocides or other substances that interfere with settlement or growth, whereas FR coatings rely on non-toxic mechanisms that allow for easy removal of fouling, with easy-to-clean or self-cleaning properties. Hybrid paints that combine both toxic and non-toxic mechanisms have also been proposed (Rittschof et al. 2008), but AF and FR paints still represent the bulk of commercial paints today (Lindholdt, Dam-Johansen, Olsen, et al. 2015).

AF paints are usually classified according to the mechanism used for biocide release, as well as the type of binder (Lindholdt, Dam-Johansen, Olsen, et al. 2015). A particularly effective type of paint, organotin-based Tributyltin Self-Polishing Copolymer (TBT-SPC), was introduced in the 1970s (Champ 2000; Yebra et al. 2004). Its success was not only due to the anti-fouling activity of the organotin compounds (e.g. tributyltin) combined with copper and other booster biocides, but it is also attributed to the unique chemical properties of the matrix, which undergo alkaline hydrolysis in contact with seawater. This reaction leads to a slow and formulation-controlled self-polishing, with preferential erosion on rough spots (self-smoothing) and biocide release even under idle conditions, i.e. zero vessel speed. Additionally, a constant and relatively thin leached layer, i.e. the uppermost layer of paint that has become practically depleted of any biocide, used to result in a practically constant biocide release rate throughout the lifetime of the paint (Yebra et al. 2004). However, TBT was later found to affect non-target marine species (Champ 2000), leading to a complete ban by the IMO. This ban is effective from beginning of 2003, for paint application in dry-dock, and 2008, for paint direct exposure to seawater on operating commercial vessels (IMO 2001). The ban on harmful antifouling coatings led to an urgent need for effective organotin-free paints, following either AF or FR principles.

Regarding organotin-free AF paints, it is useful to refer to the following main groups, even though the actual biocide-release mechanism on a given commercial product is not always clear (Yebra et al. 2004):

- Insoluble matrix paints
- Soluble matrix paints
- Controlled-Depletion Polymers (CDP) paints
- Self-Polishing Copolymers (SPC) paints (synonym: ablative paints)

Insoluble matrix paints correspond to a limited share of the market for large merchant ships (Lindholdt, Dam-Johansen, Yebra, et al. 2015), due to issues dealing with low mass transfer within a leached layer that grows over time, resulting in a rapid decay in biocide release rate (Woods Hole Oceanographic Institute 1952). Soluble-matrix paints correspond to conventional rosin-based paints, which rely on the solubility of the paint matrix to keep a more stable release rate. Upgraded CDP paints use a similar principle to that of soluble-matrix paints, with added reinforcing resins. Finally, modern SPC paints are the successors of banned TBT-SPC paints, relying on combination of Cu_2O with booster biocides for wide-spectrum action (Thomas & Brooks 2010). Still, it is questionable whether physical-chemical properties of organotin-free SPC paints can exactly mimic those of TBT-SPC paints and stand up to the same performance standard (Yebra et al. 2004).

Parallel to AF paint developments, alternative non-toxic solutions have also received significant attention from coating research and development (Swain 1999; Berntsson et al. 2000; AMBIO 2010). Non-toxic coatings rely on reduced adhesion strength through mechanical and surface properties, corresponding to most of commercially available FR coatings (Swain & Schultz 1996; Watermann et al. 1997; Brady & Singer 2000), or else rely on a micro-textured surface that inhibits settlement (Berntsson et al. 2000; Pu et al. 2016).

FR coatings usually have an initial roughness below that of AF paints, possibly leading to lower friction in newly-applied condition (Candries et al. 2003), whereas some micro-textured surfaces might even result in lower friction compared to a hydraulically smooth surface (Berntsson et al. 2000; Pu et al. 2016). However, other studies demonstrate little or no improvement in initial performance of as-applied FR coatings, thus comparable to AF coatings (Schultz 2004; Holm et al. 2004). Also, FR coatings might be unable to prevent growth on all vessels, as their success is tied to the vessel's activity and speed (Schultz et al. 2003). Finally, FR coatings are easily damaged by impact, which has consequences in

terms of lifetime and compatibility with in-water cleaning (Townsin & Anderson 2009).

FR coatings still represent a meagre share of the market, probably below 10%, with biocide-based AF coatings expected to continue dominating the market in the short term (Yebra et al. 2004; Lindholdt, Dam-Johansen, Yebra, et al. 2015). Still, the FR market is expanding, with some companies reporting gains in both economic and environmental terms (Nygren 2002).

2.2.2. In-service maintenance

Several factors may dictate an early failure of a given coating system before the end of its designated lifetime. These factors are connected with operational profile (maximum speed, speed profile and idle time), route, environmental conditions (temperature, salinity and fouling pressure), surface preparation prior to paint application, quality of paint application and history of the coating (Townsin et al. 1980; Lindner 1988; Candries 2000). Eventually, biofouling and corrosion will take over parts of the hull, greatly increasing drag (Schultz 2007).

At a given moment, costs associated with increased fuel consumption due to hull roughness justify performing in-water maintenance before dry-docking (Malone 1980; Schultz et al. 2011). Such responsive maintenance usually includes propeller cleaning and removal of fouling from selected areas of the hull, usually giving priority to the fore body of the ship, where roughness is known to cause the highest impact on ship resistance (Johansson 1984; NSTM 2006). In-water hull cleaning is commercially provided by diving companies, using a variety of technology and cleaning materials, which are selected according to the level of fouling (Morrisey & Woods 2015). By far, the most common methods applicable to large commercial vessels rely on diver-operated rotary brush carts and high-pressure or cavitation water jets. However, it is of general understanding that in-water cleaning remains a temporary solution, since it can damage sound parts of the protective coating, thus accelerating the build-up of hull roughness in the subsequent time period (Malone 1980; Munk et al. 2009). Additionally, cleaning has the potential to release biocides – chemical contamination – and viable biofoulers to the marine environment, including NIS – biological contamination. Containment techniques, e.g. filtering of debris, and chemical treatment of the effluent are both available (Morrisey et al. 2013; Morrisey & Woods 2015).

Recognizing the drawbacks of responsive in-water cleaning, proactive “grooming” has been suggested as a viable alternative, preventing the

accumulation of high levels of fouling by performing frequent and gentle in-water hull maintenance, especially after idle periods (Tribou & Swain 2010; Tribou & Swain 2015). A minimum frequency corresponding to weekly grooming events has been suggested, preventing fouling on both AF and FR coatings that were tested under static conditions in a sub-tropical estuarine environment (Tribou & Swain 2015). Cleaning frequencies higher than weekly have been suggested when using hard, non-toxic Surface Treated Composite coatings (Rompay 2013). Maintenance at such frequencies could be facilitated by remotely operated vehicles (Molland 2008), or even by future developments on autonomous underwater vehicles (Balashov et al. 2011). Still, long-term effects on specific coating systems need to be considered (Hearin et al. 2015; Hunsucker et al. 2016), together with determination of potential emissions from grooming on biocide-containing paints, which can contribute to chemical pollution (Schottle & Brown 2007; Morrissey et al. 2013).

Paper I aims at discussing in-water maintenance (hull cleaning and grooming) in light of available data on adhesion strength of marine organisms, as defined in the next section.

2.3. Adhesion strength

Adhesion strength is defined as the force per unit area (SI units: N/m²) required for removing fouling from a substrate. It can be measured using different techniques, which are selected according to the size of the fouling.

For microfouling, different experimental apparatuses have been developed, which have in common the use of hydrodynamic shear stress in testing for adhesion strength of the slime or adhered cells. These methods include the turbulent channel flow apparatus (Schultz et al. 2000), calibrated water jet (Swain & Schultz 1996; Finlay et al. 2002) and automated water jet, modified for rapid screening of fouling-control coatings (Cassé et al. 2007). For such hydrodynamic methods, the maximum wall shear stress, $\tau_{w,m}$, can be determined from direct measurements, or estimated using formulas available in the literature. The accuracy in determining the wall shear stress can affect comparison between methods, as pointed out in Paper I.

For macrofoulers, different measurement approaches are called for, due to higher adhesion strength values and size of individuals. Early methods relied on pulling forces (Crisp et al. 1985) and shear forces on rotating discs (Ackerman et

al. 1992). Most measurements are currently based on the ASTM International Standard D5618-94 (ASTM D5618 1994), which recommends the use of a handheld force gauge to determine the critical shear force, i.e. the force acting parallel to the adhesion plane required for complete removal of the individual, together with determination of the adhesion area. Based on ASTM D5618-94, variant methods have been proposed, which include the use of mesh cages for protecting macrofoulers from biotic disturbances during their growth in the field, i.e. protection from predation and grazing (Swain et al. 1998), and the later-developed reattachment assay (Rittschof et al. 2008). The reattachment assay circumvents environmental stresses, disturbances, predation and larval supply issues associated with field testing (panel immersion). In reattachment assays, barnacles are cultivated in the lab, grown on a standard surface, and then dislodged and allowed to reattach onto the test substrate. The entire procedure is thus faster and can be automated, while results compare well with field tests, as long as a 2-4 week period is allowed for the reattachment phase (Rittschof et al. 2008).

3. The rough hull penalty

This chapter gives a background on power/speed penalties due to hull roughness, with focus on biofouling roughness, as an introduction to Paper II.

3.1. Turbulent boundary layer flow

Before delving into the effects of hull roughness on ship propulsive power, a brief introduction on the viscous flow around the hull is required. For more detailed descriptions, please refer to (Schlichting 1979) on boundary layer theory, and Larsson & Raven (2010) on the viscous flow around ship hulls.

When the hull travels through water, a wall-bounded flow is created. Considering a reference point moving with the hull (Figure 3), the no-slip condition assumes that the first molecular layer of fluid has the same speed as the hull. Thus, at a null distance from the hull ($y = 0$), fluid velocity is zero in every direction (Larsson & Raven 2010b):

$$y = 0 \Rightarrow u = v = w = 0 \quad (1)$$

where u , v , and w are velocity components in the x , y and z directions, respectively (Figure 3). In this chapter, these directions correspond to longitudinal tangent (x), normal to the hull (y) and girth-wise tangential direction (z),

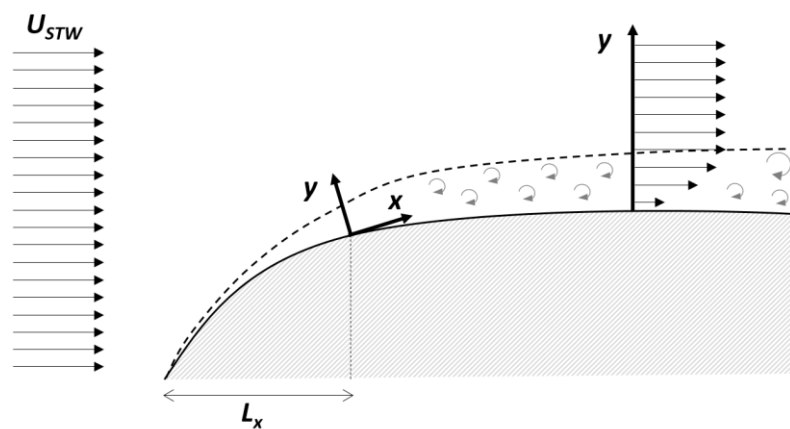


Figure 3 – Simplified representation of boundary layer flow around the fore body of a ship hull (section at constant depth). Girth-wise direction z is normal to both x and y . The bow is on the left. Only the starboard side of the hull represented.

as represented in Figure 3. Due to viscosity of the fluid, the velocity magnitude generally increases with increasing distance from the hull, giving rise to a boundary layer flow. Within the boundary layer thickness, δ , the velocity magnitude changes from zero at $y = 0$ to U_δ at $y = \delta$. It should be noted here that the speed at the boundary layer edge is not necessarily the same as the ship speed U_{STW} , which is observed sufficiently far from the hull and also in the flow approaching the ship (Figure 3). In fact, mass conservation requires that the speed at the boundary layer edge is higher than U_{STW} , due to streamlines being displaced by the hull (Larsson & Raven 2010a, p.15).

The flow around the hull is mostly turbulent (except close to the bow), meaning that velocity components change in both space and time, due to flow instabilities that arise at a high enough Reynolds number, $Re_x = L_x U_{STW} / \nu$. Close to the bow, the boundary layer changes from laminar to turbulent at a given critical value of Re_x . Downstream from that point, instantaneous turbulent fluid motions occur, which are time-dependent, as represented in Figure 3 by grey eddies.

The forces on the travelling hull can be decomposed into a frictional component, acting tangentially to the hull, and a pressure component, acting normal to the hull (Larsson & Raven 2010a). Ever since the seminal work of William Froude, friction is traditionally studied on large flat plates, whereas pressure forces due to wave-making (i.e. the wave system produced by the travelling hull) are studied on rigorously scaled models of a given hull shape. In a towing tank, flat plates are towed at the same Reynolds number as the ship, $Re_S = L_{WL} U_{STW} / \nu$, where L_{WL} is the waterline length, and scaled models of the hull are run at the same Froude number as the ship, $Fr_S = U_{STW} / \sqrt{gL_{WL}}$. However, this separation is artificial, since viscosity is known to affect wave-making resistance (Reynolds-dependency of wave patterns), and wave patterns can affect friction (Larsson & Raven 2010c). Still, provided that necessary corrections are applied, full scale resistance, R_T , can be predicted with sufficient accuracy (ITTC 2011).

Flat plate frictional resistance is obtained from *equivalent* flat plate friction, meaning that parameters such as wetted surface area S and Reynolds number Re_S are kept constant between flat plate and hull. However, the flow around a flat plate differs significantly from the hull, since there is practically no pressure gradient along the flat plate and, also, displacement effects of the flat plate can be neglected (Larsson & Raven 2010d). Thus, flat plate studies provide friction values that are independent from the hull shape, i.e. flat plate frictional resistance. Form effects must then be added to flat plate resistance, in order to estimate the

viscous resistance on the hull. Viscous resistance includes both *form effects on friction*, caused by a higher speed at boundary layer edge due to hull displacement of streamlines at the bow, and *form effects on pressure*, caused by reduced pressure on the aft body due to boundary layer displacement of streamlines at the aft (Larsson & Raven 2010a). These form effects are addressed in Paper II, using the so-called form factor, K .

3.2. Flow over rough surfaces

So far, a smooth hull has been considered. However, since the flow around the hull is mostly turbulent, wall roughness becomes an important parameter to consider, as the protrusion of roughness elements will eventually result in increased turbulent kinetic energy and increased wall shear stress (Lee 2015).

First of all, the presence of roughness elements renders impossible to establish an unequivocal positioning of the y -origin, as Figure 4 represents. Thus, the y -origin is arbitrarily set at the highest roughness peak and a wall origin error ε is added (fitted parameter), defining the distance from the wall as $y + \varepsilon$ (Lewthwaite et al. 1984; Perry & Li 1990; Cal et al. 2009).

The following discussion concerns a boundary layer over a flat plate, with zero pressure gradient. On inner-scaled velocity profiles, where wall shear velocity $u_\tau = \sqrt{\tau_w/\rho}$ is used as velocity scale ($u^+ = u/u_\tau$) and ν/u_τ as length scale ($(y + \varepsilon)^+ = (y + \varepsilon)u_\tau/\nu$), several regions can be identified (Cal et al. 2009; Larsson & Raven 2010d):

- For $(y + \varepsilon)^+ < 5$, there is a viscous sub-layer (also called linear sub-layer), where u^+ varies linearly with $(y + \varepsilon)^+$:

$$u^+ = (y + \varepsilon)^+ \quad (2)$$

- For $5 < (y + \varepsilon)^+ < 30$, a buffer layer exists, where the profile gradually changes from linear to logarithmic.
- A logarithmic region follows, for $(y + \varepsilon)^+ > 30$:

$$u^+ = \frac{1}{\kappa} \ln[(y + \varepsilon)^+] + C - \Delta U^+ \quad (3)$$

where κ is the von Kármán constant, C is the smooth intercept and ΔU^+ is the roughness function, which varies from $\Delta U^+ = 0$, for hydraulically smooth flow, to $\Delta U^+ > 0$, for hydraulically rough flow.

- For still higher values of $(y + \varepsilon)^+$, an outer layer (or wake region) can be found, where the wake parameter Π_i is included:

$$u^+ = \frac{1}{\kappa} \ln[(y + \varepsilon)^+] + C - \Delta U^+ + \frac{\Pi}{\kappa} \left[\sin \left(\frac{\pi y + \varepsilon}{\delta} \right) \right]^2 \quad (4)$$

Having introduced the different regions of the turbulent boundary layer in inner-scaled velocity profiles, roughness effects are usually noted in the logarithmic region by a downward shift in velocity profiles, $-\Delta U^+$. Parameter ΔU^+ is a function of Reynolds number based on roughness height, $k_t^+ = k_t u_\tau / \nu$. For low k_t^+ , the flow is said to be hydraulically smooth and $\Delta U^+ = 0$. In this regime, the flow turbulence caused by roughness elements is completely dampened by viscosity (Flack & Schultz 2014). For higher k_t^+ values, different roughness geometries will result in different curves $\Delta U^+ = \Delta U^+(k_t^+)$, since k_t is only one of many roughness parameters that characterize the surface (Grigson 1987; Candries & Atlar 2005; Flack & Schultz 2014). This mismatch is exemplified in Figure 5, where the two most commonly-used roughness functions are shown, namely Nikuradse's uniform sand roughness function (Nikuradse 1933) and the Colebrook-type roughness function (Johansson 1984). The onset of roughness effects differs between the two functions: a sharp onset for Nikuradse's function at $k_s^+ = 5$, where k_s refers to the roughness height of uniform sand grains used in Nikuradse (1933), compared to an asymptotic behaviour $\Delta U^+ \rightarrow 0$ for decreasing k_s^+ in the Colebrook-type function (Figure 5). Accordingly, Nikuradse's roughness function is steeper in the transitionally rough regime, i.e. for $5 < k_s^+ < 90$ (Cebeci & Bradshaw 1977).

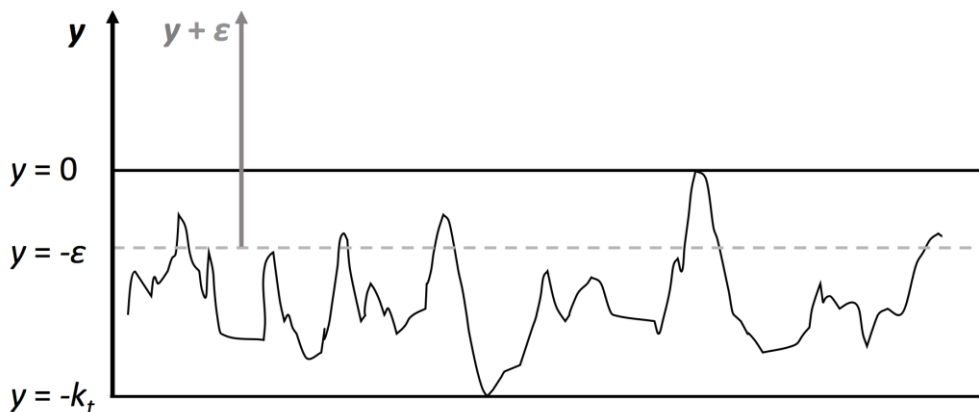


Figure 4 – Arbitrary roughness profile, peak-to-valley roughness height k_t , and the concept of virtual origin, where ε is the wall origin error.

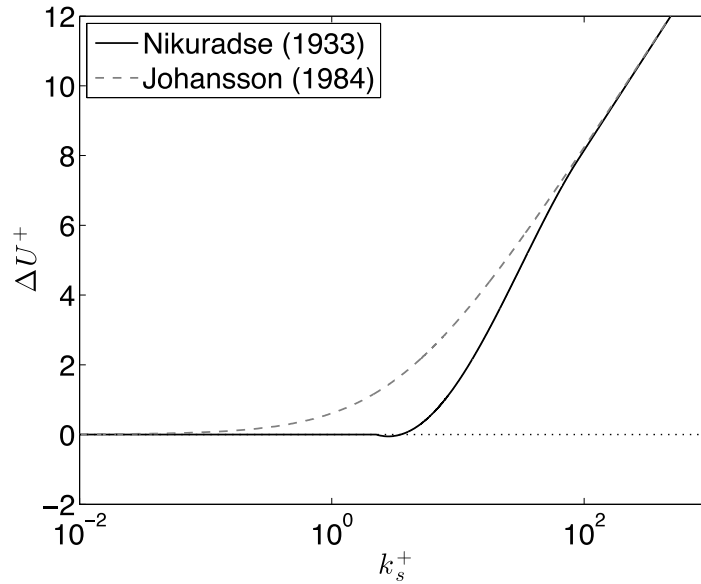


Figure 5 – Two examples of roughness functions: Nikuradse’s uniform sand roughness function (Nikuradse 1933) and Colebrook-type roughness function (Johansson 1984).

Regardless of surface topography, ΔU^+ shows the same asymptotic linear behaviour for sufficiently high k_t values (Figure 5, $k_s^+ > 90$). This is associated with fully rough behaviour and a Reynolds-independent local friction coefficient C_f in Moody-type diagrams (Flack & Schultz 2014). Thus, in the fully-rough regime, it is possible to define an equivalent roughness height for each surface, effectively collapsing all roughness functions into one fully-rough asymptote, usually reporting back to Nikuradse’s uniform sand roughness k_s as a “common currency” (Cebeci & Bradshaw 1977; Bradshaw 2000; Flack & Schultz 2010). Thus, in the fully-rough regime, ΔU^+ is a linear function of $\ln k_s^+$:

$$\Delta U^+ = C - 8.5 + \frac{1}{\kappa} \ln k_s^+ \quad (5)$$

Using the above expression, the equivalent roughness height k_s can be obtained experimentally for any roughness type of interest. Subsequently, correlations can be sought between k_s and surface topography parameters, such as percentage cover (Schultz 2004).

3.3. Previous drag research

Drag research on biofouling dates back to at least 1915, when McEntee studied flat plates covered with “small barnacles” (Woods Hole Oceanographic Institute 1952). Since then, different methods have been used, including local boundary layer measurements on the hull, towed flat plates, rotating equipment with torque meters, pipe flow methods and channel flow facilities. Main conclusions from more recent studies are summarized here, in a non-exhaustive way.

In the 1980s and 1990s, different studies looked at local effects of biofouling, namely using a velocity probe directly projecting from a ship’s hull (Lewthwaite et al. 1984), velocity measurements in water tunnels (Johansson 1984; Schultz & Swain 1999) and friction measurements using rotating disks, together with sea trials (Haslbeck & Bohlander 1992). It was found that slimes, ranging from a thin layer of slime only detectable by touch to a dense 1-mm thick slime, were responsible for increases of 25-80% in local skin friction coefficient C_f (Lewthwaite et al. 1984). Later measurements on microfouling using a rotating disk setup led to similar conclusions, with drag penalties in the range 9-29% (Holm et al. 2004). Also, water tunnel measurements demonstrated a 33-187% increase in C_f for marine biofilms compared to a smooth reference, depending on biofilm thickness and morphology (Schultz & Swain 1999). It should be noted here that each of these C_f values still tied to the Reynolds number of each experiment.

Concerning more advanced stages of biofouling, a barnacle-covered surface with $k_t = 5$ mm caused an increase in C_f of almost 280%, compared to the same surface after removal of the barnacles down to their basal plates, which still exhibited a k_t of 650 μm (Johansson 1984). Again, it should be noted that C_f is still tied to the Reynolds number of the experiment. More recently, a useful formula has been suggested for relating the equivalent sand roughness height k_s , which is independent of Reynolds number, to two geometrical parameters, namely the height of the largest barnacles (k_t) and the percentage barnacle cover (Schultz 2004):

$$k_s = 0.059 \times k_t \times (\% \text{ cover})^{0.5} \quad (6)$$

Filamentous-type roughness, corresponding to macroalgae such as *Ulva* sp. (synonym: *Enteromorpha*), was first investigated using nylon tufts (Lewkowicz & Das 1986) and later on with algae-covered panels (Schultz 2000; Gangadharan et al. 2001; Subramanian et al. 2004). An increase in local C_f of 110-125% was measured for filamentous algae compared to a smooth reference, exhibiting a

mean algal layer thickness of 3.8–6.4 mm, as measured under flow conditions (Schultz 2000). There is a difficulty in defining a characteristic length scale for filamentous-type roughness, considering that the surface roughness is flow-compliant (pliable under flow) and therefore more complex to characterize than a surface roughness that is not altered by the flow (Schultz 2000; Townsin 2003).

Recently, hydrodynamic tests have been conducted on dynamically immersed surfaces, using rotors on an ocean-placed raft (Lindholdt, Dam-Johansen, Olsen, et al. 2015), using large rotating disks in the field (Hunsucker et al. 2016), or using cultivating facilities in the lab (Schultz et al. 2015; Yeginbayeva et al. 2016). The frictional drag of microfouling samples was not significantly affected by the hydrodynamic stress during cultivation (Hunsucker et al. 2016) or by the fact that slimes were grown under natural or laboratory conditions (Yeginbayeva et al. 2016). Biofilms composed of diatoms were responsible for up to 70% increase in C_f , but no relation could yet be found between hydraulic k_s and physical roughness parameters, such as roughness height and percentage cover (Schultz et al. 2015).

Finally, considering that the experimental determination of hydrodynamic parameters such as k_s is costly, alternative procedures have been suggested, such as manufacturing of solid roughness coupons based on a scan of fouled surfaces, enabling to use more simple and widely available wind-tunnel facilities (Monty et al. 2016).

Alternatively, *in situ* velocity profile measurements through a window on the hull would enable studying the boundary layer flow around the ship using Laser Doppler Anemometry (Hutchins et al. 2016), following the same basic idea as first suggested in Lewthwaite et al. (1984). The main limitation of the later measurements is that these only represent local effects of roughness, not to mention practical constraints in implementing and maintaining the system, namely the need for installing a system through the hull, and avoiding fouling of the window for flow visualization.

3.4. Full scale roughness effects

Local roughness effects only give us a hint on potential friction penalties caused by biofouling and mechanical hull roughness. Thus, further methods are required for estimating penalties at the ship scale.

3.4.1. *From lab to ship*

As seen in Section 3.2, the equivalent roughness k_s and function $\Delta U^+ = \Delta U^+(k_s^+)$ are hydraulic parameters that completely characterize roughness effects on wall-bounded flows. However, k_s and $\Delta U^+ = \Delta U^+(k_s^+)$ need to be determined experimentally for the roughness topography exhibited on the hull, or using correlations that take into account a number of roughness parameters, or surface statistics (Ünal et al. 2012; K. a. Flack & Schultz 2014). Additionally, accurate and detailed characterization of the hull surface on a floating vessel, or even on a dry-docked vessel, faces severe practical constraints, not the least of which the mammoth scale of most commercial vessels. In fact, only linear profilometers and simple correlations for predicting power are routinely used today for painted hulls in the dry dock (Townsin 1991; Carlton 2007). Admitting that practical constraints can be overcome, k_s and $\Delta U^+ = \Delta U^+(k_s^+)$ enable to calculate full-scale penalties, using one of several available numerical methods.

The most simple and time-saving method for scaling-up consists in calculating the frictional resistance of a rough flat plate equivalent to the ship in question, using an extrapolation method based on Granville's similarity law scaling (Schultz 2007). As mentioned above, such equivalent flat plate is defined as having the same length and wetted surface area as the ship, and travelling at the ship's Reynolds number, Re_s . Each calculation currently takes about 0.1 seconds on a laptop computer and, thus, a large number of cases can be evaluated. However, this approach has its limitations: (i) the hull is assumed to be uniformly covered with a certain roughness, which is rarely the case on a real ship; (ii) hull form effects on the roughness component of resistance are not considered, as the increased resistance on a flat plate can differ from that of the hull shape.

Advances in Computational Fluid Dynamics (CFD) enable full-scale simulations of the flow around the ship (Leer-Andersen & Larsson 2003; Raven et al. 2008; Castro et al. 2011; Demirel et al. 2017). In principle, such codes would allow for an inhomogeneous roughness distribution on the hull, which would better represent real ships (Demirel et al. 2017). However, the computational cost of such simulations is much higher than the extrapolation method based on Granville's similarity law scaling (Schultz 2007). Also, practical challenges associated with obtaining k_s and $\Delta U^+(k_s^+)$ for each region of the hull, as pointed out before, do not currently justify a more detailed approach than more simple extrapolation methods, such as Granville method (Schultz 2007).

3.4.2. Monitoring approaches

The impact of a rough hull on energy efficiency is well recognized by ship managers. However, early detection of a failed underwater hull coating is still a challenge, due to numerous factors affecting the quality and quantity of in-service vessel performance data (logged data) and the limited amount of information that can be obtained from sporadic underwater surveys.

In-service performance data can be obtained from manual and/or automatic reports from the ship's bridge and engine room (Carlton 2007). Several relevant parameters can then be analysed according to different methods, which range from simple power-speed curves (Ricketts & Hundley 1997) to more advanced algorithms that seek to isolate the effect of hull and propeller roughness (Pedersen 2015; ISO 2016). However, the usefulness of the results will still be dependent on sensor accuracy, measurement frequency and modelling errors associated with corrections for draft, trim, waves, wind, sea currents, temperature and salinity (Carlton 2007; Munk et al. 2009; ISO 2016). Regarding environmental corrections, the spread in the results can be diminished by using high-frequency data, and by filtering out data points according to certain criteria (ISO 2016) or other type of outlier analysis (Meng et al. 2016).

Finally, underwater surveys are used by the U.S. Navy for determining the Fouling Rating, ranging from FR-0 to FR-100 for increasing degree of fouling (NSTM 2006). This Fouling Rating, complemented with simple performance criteria concerning attained speed and required shaft revolutions, can be used as a trigger for underwater maintenance. For instance, a vessel coated with SPC paint and exhibiting a level of fouling of at least FR-40 (tubeworms < 6.4 mm in diameter or height) on 20% of its hull area⁵ would be eligible for a full hull cleaning (NSTM 2006). Such guidelines result from specific economic considerations and probably do not apply to other types of vessel. Still, other operators might be able to follow similar approaches, considering advances in both *in situ* measurement technology and understanding of biofouling hydrodynamics (Schultz et al. 2015).

⁵ Excluding dry-docking support strips and appendages (NSTM 2006)

THE ENEMY BELOW

4. Discussion

4.1. Marine fouling adhesion

As presented before, fouling control coatings eventually lose their effectiveness, resulting in a fouled hull, increased hull surface roughness and, consequently, propulsive power penalties. This would hopefully occur only towards the end of the dry-docking interval, not too long before the paint system can be repaired. Otherwise, fuel economy calls for responsive in-water cleaning (Malone 1980). In alternative, hull grooming has been suggested, in the form of proactive and gentle cleaning procedures (Tribou & Swain 2010). This section discusses both types of maintenance, in the light of adhesion strength values for different marine fouling organisms, as reviewed in Paper I.

The aim of any in-water hull cleaning method is to remove growth without damaging the underlying paint system, which might include sound layers of AF coating still containing biocides that can protect the hull from further fouling in the subsequent time period, or the FR coating, whose surface properties should be kept in order to weaken the adhesion of subsequent potential settlers. Curiously, this aim has been compared to that of toothbrushes, which should enable to clean teeth without damaging the soft gums (Holm et al. 2003). Thus, aiming at matching in-water cleaning forces with the minimum force necessary to remove fouling, values of adhesion strength of both micro- and macrofoulers on ship hull coatings have been collected in Paper I, from available literature.

For macrofouling, values of adhesion strength on epoxy primers, AF and FR coatings corresponded to 0.3–2.2 MPa, 0.5 ± 0.2 MPa (only one AF coating) and 0.03–0.5 MPa, respectively. As expected, the epoxy used for corrosion protection is generally associated with higher adhesion strength, followed by an AF coating and, finally, FR coatings. Surprisingly, only one value could be found for adhesion strength of barnacles on an AF coating, since the overwhelming majority of adhesion strength tests actually aim at screening/comparing different FR solutions, as discussed in Paper I. Besides the substrate, adhesion strength of macrofoulers may depend on the species, geography, season and other variables. Nevertheless, the above adhesion strength values are well above the cleaning force exerted by a specific brush grooming tool on instrumented studs representing barnacles, which corresponded to approximately 0.01 MPa (Holm et al. 2003; Tribou & Swain 2015). Thus, more aggressive cleaning methods are required, leading to two potential issues: (1) occurrence of cohesive failure, in

which the organism's shell is destroyed before reaching the force necessary for complete removal of the shell, leading to a surface covered with shell residues that can serve as cue for subsequent settlers; (2) damage to fouled, unfouled or already cleaned areas of the paint. Thus, responsive cleaning is discouraged, in favour of hull grooming performed at an earlier stage. However, responsive cleaning can still be a good option when an AF coating is not yet completely depleted, i.e. when it can be proven that sound layers of AF coating still exist beneath the fouling and an eventual leached layer (layer depleted of biocide). In that case, the cleaning would have the effect of increasing the biocide release rate, i.e. the paint is reactivated, approaching its initial effectiveness. This is however made at the cost of local discharge of biocides and paint residues (Schottle & Brown 2007; Earley et al. 2014) and it can still affect sound layers of AF paint (Morrisey et al. 2013). It should also be noted that FR are usually more sensitive to aggressive cleaning methods than AF coatings, and the subsequent effectiveness of FR might get compromised after such cleaning events (Townsin & Anderson 2009).

For microfouling, collected values of adhesion strength on FR coatings were in the range 8-275 Pa, for removal of at least 80% of the initial fouling. No values could be found for adhesion strength of microfouling on AF coatings. It should be noted that adhesion strength depends not only on the substrate and criterion for percentage removal, but also on the species, stage of development (adhered cells, biofilm, sporelings...) and exposure time to shear stress (cleaning time), as well as numerous environmental variables. Nevertheless, these values already give an indication of how low forces are required to remove microfouling. Thus, more gentle cleaning methods, such as grooming tools, can be used for removing such fouling (Tribou & Swain 2015), although tenacious biofilms have been recorded, which could not be removed by a grooming brush tool (Hearin et al. 2016). Considering this tool exerts approximately 0.01 MPa on instrumented studs (Holm et al. 2003; Tribou & Swain 2015), this failure to remove tenacious biofilms suggests that the cleaning forces acting on low-profile roughness (coated or microfouled surfaces) might be lower than those measured on instrumented studs, or else the adhesion strength of tenacious biofilms is higher than the above reported values for microfouling.

The methods used for measuring adhesion strength are also discussed in Paper I. For testing macrofoulers, it is highlighted the need for reporting the occurrence of cohesive failure, e.g. as a percentage of discarded measurements due to shell breakage. This is important, since adhesion strength is probably underestimated when cohesive failure becomes more frequent, as only the

weakly attached individuals are pooled (assuming that the shell strength does not vary widely between individuals). For hydrodynamic testing of microfouling, differences in the method of estimation of wall shear stress may be responsible for differences between studies, besides all other factors already mentioned above.

Finally, it should be added to the discussion of Paper I that there is a risk associated with underestimating the adhesion strength of biofouling: a too low cleaning force could be selected, resulting in a need for re-cleaning the surface after stepping up the cleaning force, thus wasting precious time available for the job, already constrained by the vessel's schedule. One solution for this would be to select a representative area of the hull for conducting preliminary testing of cleaning forces.

4.2. Triggers and maintenance assessment

In the previous section, the aspect of adhesion strength has been discussed, as well as its implications for in-water cleaning (Paper I). The question that follows suit corresponds to *when* to perform in-water cleaning. The answer is not at all trivial, as a number of aspects must be considered, not the least of them the route and time constraints associated with a trading vessel. Besides route and time constraints, important aspects correspond to the hydrodynamic performance of the hull, cost of cleaning and potential shortening of subsequent lifetime of the paint. This sub-section focuses on the first, hydrodynamic performance, as directly related to the impact on fuel consumption (Paper II).

As introduced in Chapter 3, Paper II discusses prediction methods for the fouled hull resistance penalty, ΔR , using as input the roughness function and the equivalent sand roughness height associated with a given hull surface condition. In principle, such methods can be used in estimating power penalties, ΔP , and derive conclusions regarding cleaning in a fuel-economy perspective, as long as the propulsive coefficient, η_D , is known or estimated (Schultz 2007), since shaft power P is related to resistance R_T and vessel speed U_{STW} by:

$$P = R_T U_{STW} / \eta_D \quad (7)$$

The novelty introduced by Paper II corresponds to the accounting for form effects on rough hull friction, as well as other viscous effects, i.e. viscous pressure resistance, considered to be a function of friction (ITTC 2011). This means that increased resistance due to roughness is expected to be higher on a hull than on

its equivalent flat plate. The deviation in viscous resistance from a flat plate is quantified by the form factor K , which is lower for more slender hulls.

In order to test the form factor hypothesis, it is necessary to obtain resistance results for a given ship at both smooth and fouled hull conditions, together with results for the equivalent flat plate. A very recent numerical study provides exactly such results for a containership: Demirel et al. (2017) used CFD to simulate the towing resistance of the KRISO container ship (KCS) in calm waters, for different hull roughness conditions, and the same paper also provides CFD results for the equivalent flat plate using the same numerical method. Change in total resistance coefficient due to roughness, ΔC_T , was derived from those results and is here plotted in Paper II – Fig. 2. It is observed that, for 19 knots, results for the hull shape (KCS hull) are always 5-8% higher than for the equivalent flat plate (Paper II – Fig. 2a). This agrees fairly well with a form factor of ~10% for the KCS hull, i.e. $K = 0.1$ (Castro et al. 2011). Results for 19 kn thus support the hypothesis of a form effect on roughness penalties. The same conclusions cannot be drawn from simulations at a higher speed of 24 kn, with differences between KCS hull and flat plate varying between -5% and +4% (Paper II – Fig. 2b). In Paper II, this null form effect is shown to be due to cancelling effect of a decrease in wave-making resistance with increasing hull roughness, as observed by the authors of the original data (Demirel et al. 2017).

According to Paper II, the form factor hypothesis cannot be generalised for all speeds, due to viscous effects on wave-making resistance. Still, form effects on hull penalties might be significant at low speeds (wave-making resistance corresponding to $\leq 12\%$ of total resistance) and for vessels associated with a high form factor K , e.g. tankers, which are typically less slender than containerships. Different approaches were compared in Paper II, and the Granville method (Schultz 2007), without any correction for form effects, provided reasonably accurate results when compared with the CFD results for the KCS hull (Paper II – Fig. 3).

The approach followed in Paper II assumes the hull as uniformly covered with a constant value of equivalent sand roughness height. Since the hull is usually not uniformly rough, this approach represents, at best, an *average* hull roughness. Also, the approach is based on experimental measurements on surfaces as similar as possible to those observed on the hull. This leads to a methodological issue, as discussed below in Section 4.3, since the actual hull condition can be only approximately matched with existing experimental studies, as it is certainly impracticable to experimentally test every existing hull condition.

Instead, an alternative application of the Granville method (Schultz 2007) is here proposed, which combines the Granville method with vessel performance data, similar to that used in ISO 19030 (ISO 2016).

By iteratively applying the Granville method, as shown schematically in Figure 6, the average equivalent sand roughness height of the hull can be estimated at each point in time, i.e. $k_s(t)$. The procedure includes three main parts: (1) collection, validation and filtering of monitored data, together with external information on the ship, i.e. vessel specifications, hydrostatic data and power-speed relations for a clean hull, as in ISO 19030 (ISO 2016), (2) calculate power increase due to hull roughness, i.e. the difference between measured and expected power, and (3) finding the value of k_s that yields the same ΔP within a certain tolerance, using the Granville method to obtain ΔR iteratively, using some method for estimating the propulsive coefficient or assuming a constant propulsive coefficient. Finally, $k_s(t)$ can be used in determining the power-speed relation at different speed and loading conditions for assisting the decision of *when* to perform in-water hull cleaning. This can be done by defining a *trigger* for in-water hull cleaning, i.e. a maximum allowed value for k_s , which would be specific for a given vessel and operational profile; alternatively, potential gains from hull grooming can be evaluated. Other economic aspects then come into play, namely the cost of each maintenance event, as well as the expected effectiveness of the paint after each maintenance event.

The main advantages of estimating equivalent roughness height from vessel performance data consist in that, in principle, the obtained k_s represents the average roughness condition of the hull and k_s is independent from vessel speed. In fact, it has been noted before that reporting hull performance in terms of percentage change in speed (or, alternatively, percentage change in power), is still speed-dependent, as at higher speeds wave-making resistance increases and roughness-dependent viscous resistance becomes less important (Bertram 2017). Additionally, k_s results can be used in estimating the required power for any given vessel speed. Disadvantages include uncertainties from the monitored vessel data, external data, input errors and modelling errors. The later include input and modelling errors in flat plate resistance and determination of propulsive coefficient, η_D . These and other aspects are further explored in section 4.3 Methodology.

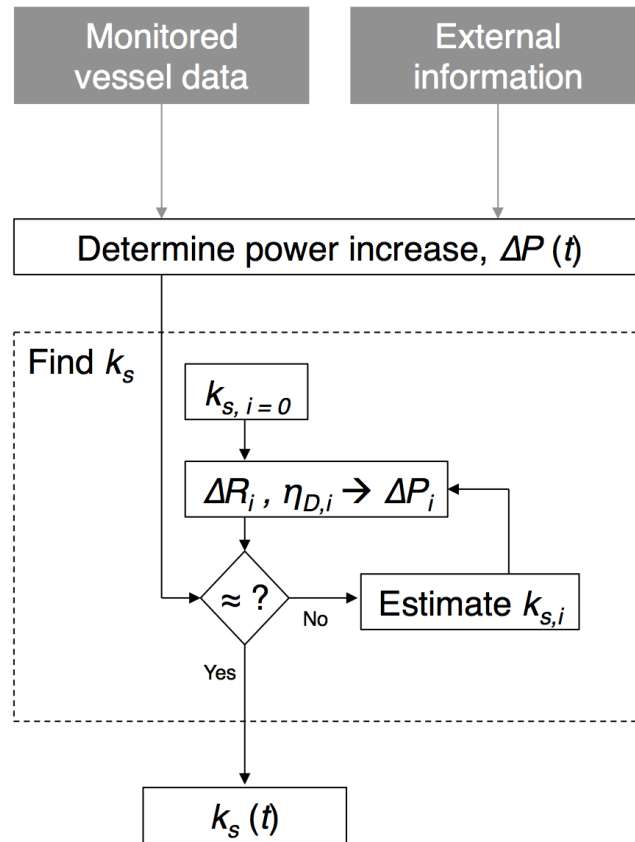


Figure 6 – Alternative iterative procedure for applying the Granville method, where the Granville method calculates resistance penalties (ΔR), given a certain hull roughness condition (k_s), which can be translated into fuel penalties (ΔP) after estimating the propulsive coefficient (η_D).

As an example of application of this iterative procedure (Figure 6), noon reports are used here, which were kindly provided by the shipping company collaborating in the project. The data correspond to a tanker, whose main specifications are given in Table 1. Raw data from noon reports, spanning a period of more than 3 years, was imported to Matlab. The data starts ~8 months after the last dry-docking of the vessel for periodic hull maintenance (exactly 254 days). Data points associate with high wind speeds (>7.9 m/s) and vessel speed outside the sea trial power-speed curves were filtered out (ISO 2016). No other filters or corrections were applied. Propulsive coefficient η_D was kept constant (Svensen 1983, pp.49–61), as derived from model test data. Results are presented in Figure 7, for percentage speed loss and vessel speed. Vertical lines

indicate cleaning events, including diver-operated brush carts and propeller polishing. No dry-dockings occurred during the sampling period. In Figure 7, it is observed that speed loss is generally lower after a cleaning event, but there is still some dependency on speed: the lower the vessel speed, the higher the speed loss. By using the iterative procedure outlined in Figure 6, k_s results can be obtained as shown in Figure 8, where k_s is plotted as a function of time. It should be noted that, in Figure 8, the scale for the k_s axis is logarithmic, and that significant amplitude in hull roughness of 2-3 orders of magnitude is observed in the 3.5-year period.

Remarkably, k_s results in Figure 8 are generally not far from those estimated from divers' inspection reports, as represented by coloured plus signs. As an estimate for the hull condition after cleaning (green plus signs), a deteriorated AF coating was assumed, corresponding to $k_s = 100 \mu\text{m}$ (Schultz 2007). The results obtained using the iterative procedure from Figure 6 seem to agree well with estimates from inspections, and the effect of cleaning events can be noted in most of the cases. Two exceptions are noted for inspections carried out around 2.5 – 3 years, which were reported by two diving companies with different inspection protocols from the rest. For obtaining k_s based on diver inspections before cleaning (red plus signs), maximum barnacle height and percentage cover were used as inputs to Equation 6 (Chapter 3). Furthermore, it should be noted that the low sampling frequency (noon reports) might not be compatible with a prompt trigger for cleaning events, especially considering that part of the data points is filtered out due to high winds (used as proxy for rough weather and waves) or out-of-range vessel speed, dropping the frequency to less than daily. Higher sampling frequency than noon reports would yield more data points, but the spread in the results would still remain, as observed already in Figure 8, e.g. around $t = 0.5$ years, where oscillations within ~ 1 order of magnitude are noted. The procedure might yield better results if the quality of the data would be more closely checked, more reference power-speed-draft-trim curves would be used and corrections for relative wind introduced (ISO 2016).

Table 1 – Main vessel specifications for a tanker.

Year Built	2008
Waterline length L_{WL}	222.96 m
Displacement ∇	74,329 m ³
Draft T	12.20 m
Breadth B	32.25 m
Block coefficient C_B	0.847 –
Wetted surface area S	10,997 m ²
Design speed U_{STW}	14.00 kn
Shaft power P at design speed	7,164 kW
Propulsive coefficient η_D at design speed	0.600 –

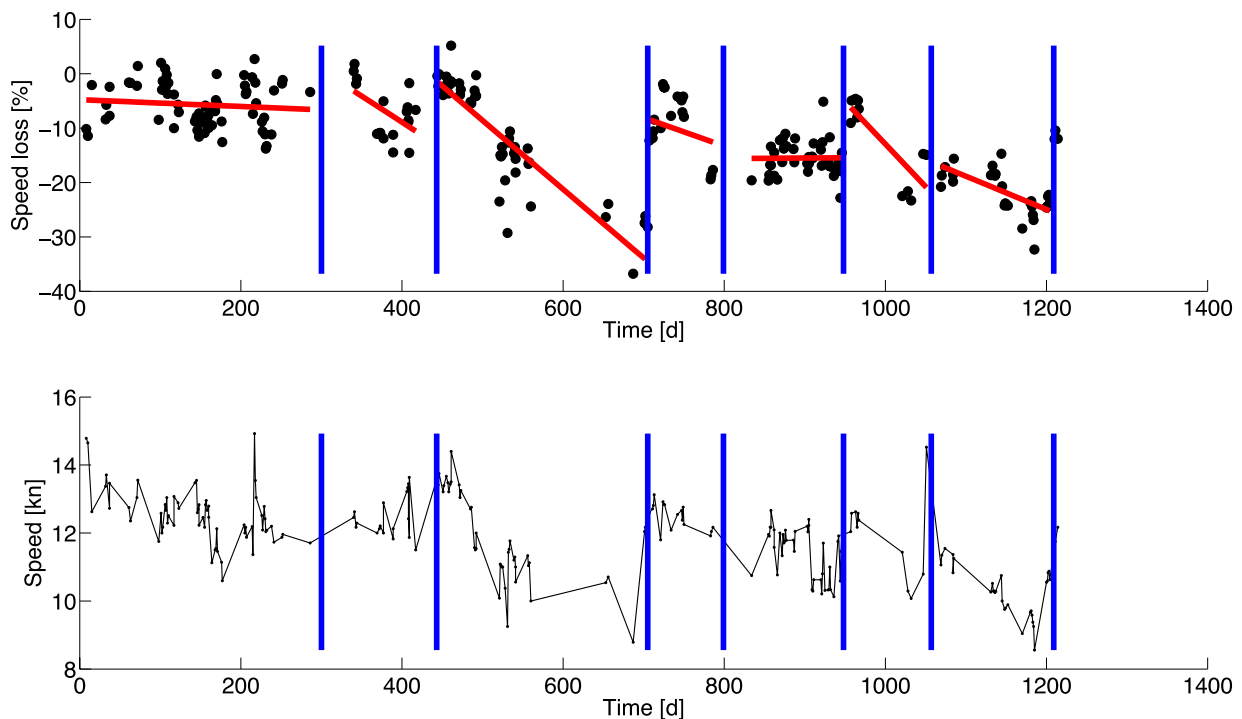


Figure 7 – Speed loss and measured speed through water for a tanker in a period of 3 years. Hull and propeller cleaning events are marked with vertical lines.

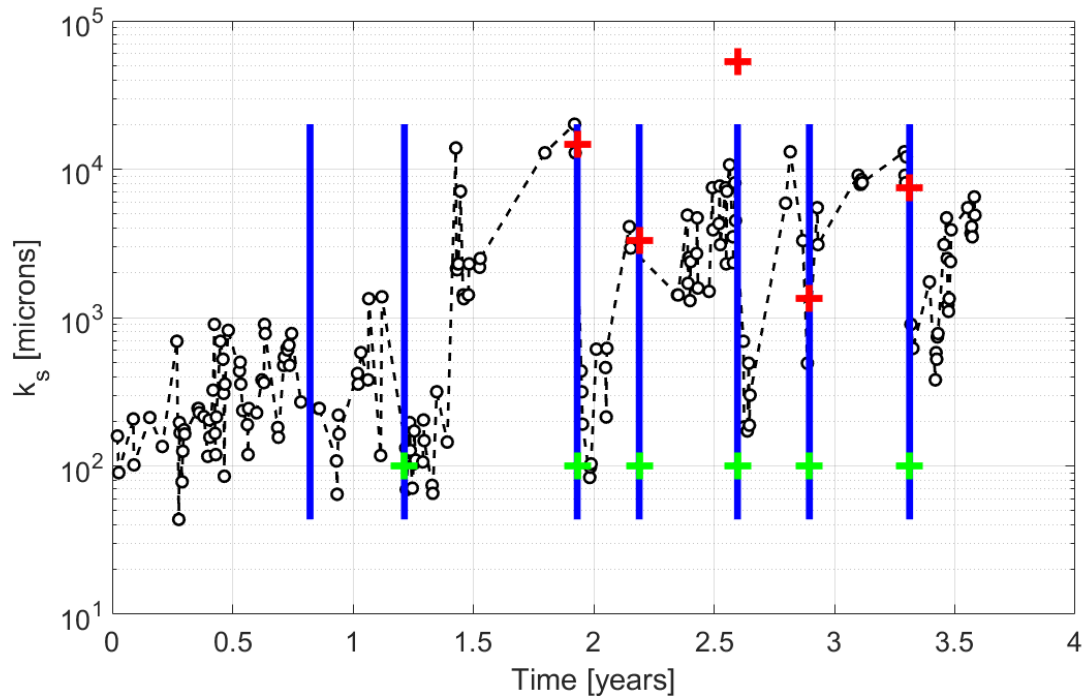


Figure 8 – Evolution of equivalent sand roughness height for a tanker in a period of 3 years. Hull and propeller cleaning events are marked with vertical lines. Estimated equivalent roughness before cleaning (red plus signs) was calculated from divers' reports (Chapter 3, Equation 6), while equivalent roughness after cleaning (green plus signs) were estimated as $100\ \mu\text{m}$, assuming a deteriorated coating (Schultz 2007).

Finally, k_s values from the above tanker can be converted to percentage increase in resistance ΔR [%] for the same tanker travelling at constant speed and draft, say 14 kn and 12.2 m, respectively (Figure 9). This quantity, ΔR [%] for a specific speed and draft, is also independent from the *actual* vessel speed. The slopes of linear regression within each period between cleaning events is seen to generally increase with time, which is in agreement with possible damage to the AF coating. On the same in Figure 9, the cumulative number of days idle is shown by a green line, which might further help explaining some of the features of ΔR : (1) a slow increase in resistance before the first cleaning might be partially due to short idle periods; (2) a long idle period of ~ 3 months between $t = 540$ and 730 days most probably contributed to exacerbate the growth; (3) an idle period of ~ 1 month right after the 4th cleaning event probably lead to almost no apparent effect of that cleaning event on hull performance; (4) before the last cleaning event, the slope is again less steep, which coincides with comparatively shorter idle periods. The importance of idle periods on biofouling penalties cannot be overstated, since idle periods allow biofouling settlement, especially towards the end of the dry-docking interval, when the AF coating starts to fail.

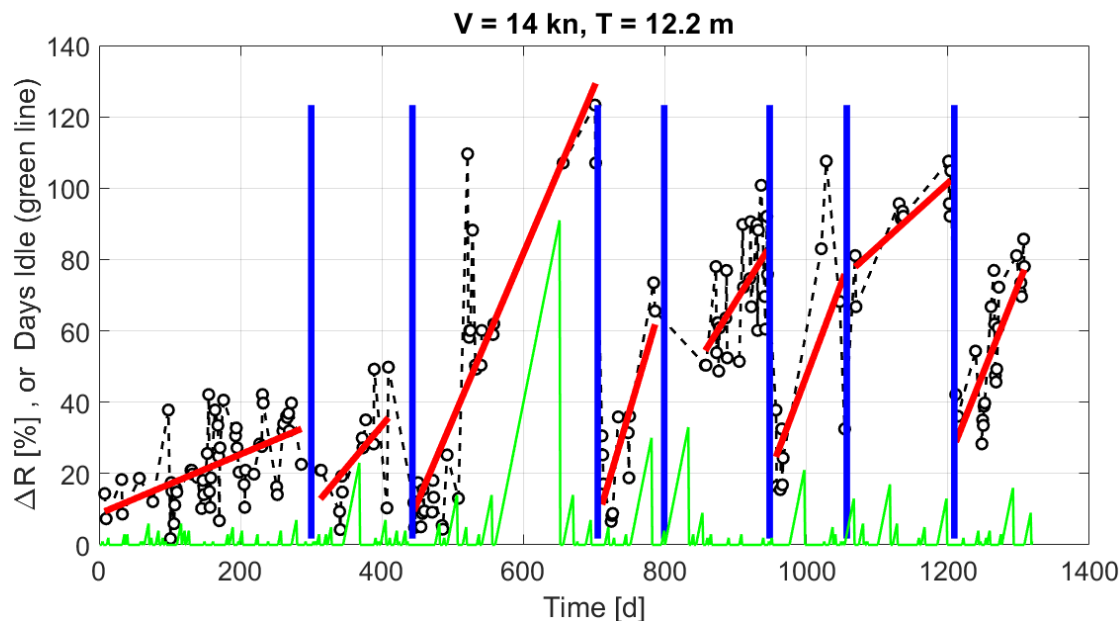


Figure 9 – Increase in resistance ΔR [%] relative to a hydraulically smooth hull (circles), and idle time (green line), for a tanker in a period of 3 years. Hull and propeller cleaning events are marked with vertical lines. Reference speed and draft correspond to 14 kn and 12.2 m, respectively.

4.3. Methodology

In the on-going project, optimization of hull maintenance regarding both forces and frequency is aimed at. The current section discusses the methodology used towards this aim.

In Paper I, adhesion strength values obtained from literature are reviewed, aiming at matching cleaning forces with required force for biofouling removal and thus minimizing damage to the hull coating. First of all, it should be noted that, although expressed in the same units of force per unit area, adhesion strength values are not directly comparable between micro- and macrofouling, as forces are estimated from hydrodynamic relations in the first case and directly measured with force gauges in the second case. Also, actual forces imparted by cleaning tools must be obtained using methods that enable useful comparisons: e.g. the force exerted by a brush grooming tool on instrumented studs representing barnacles (Holm et al. 2003; Tribou & Swain 2015) can be directly compared to force gauge measurements on real barnacles, assuming that there are no significant scale effects, i.e. the size of the real barnacles is comparable to that of the instrumented studs. For microfouling and coated surfaces, other methods

are required for determining cleaning forces exerted by any given cleaning tool. Such methods should be adapted to the significantly lower roughness height of such surfaces. For example, cleaning tools using water jets (or other hydrodynamic methods) enable the user to estimate cleaning forces at the surface level (pressure and wall shear stress) using simple hydrodynamic relations or CFD simulations of the cleaning apparatus. Such methods should be further investigated and validated. Only then can the currently discussed adhesion strength values for microfouling become truly useful.

The methods discussed in Paper II for determining fuel penalties due to hull roughness are intended to provide some basis for decisions on when to perform in-water maintenance. However, as mentioned before, such methods require experimental testing on a sample of the actual hull roughness. Also, some of these fail to represent the non-homogeneous distribution of roughness on the hull, contributing to uncertainties. Thus, a methodological issue arises, in which the practical goal of estimating propulsive power penalties for a given ship is hindered by the lack of information on the roughness function and average roughness height associated with each particular case (hull condition).

The procedure suggested in the previous chapter for solving this methodological issue consists in combining vessel performance data collected from the ship with a scaling-up method such as the Granville method (Schultz 2007), used here iteratively to find k_s for a given ΔP (Figure 6), i.e. estimating the cause from the observed effect. Thus, k_s represents the equivalent sand roughness height, uniformly distributed on the hull, which would be responsible for the actual penalty ΔP , assuming a *clean propeller*. The fact that k_s is obtained assuming a clean propeller means that the effects of hull and propeller roughness cannot be analysed separately. Still, there is significant advantage in the fact that k_s can be used as a measure of hull performance that is independent from the vessel speed, which is not the case with previously suggested indicators, such as percentage speed loss (ISO 2016; Bertram 2017). The approach can be applied to any vessel, as long as sufficient technical details and data are available. Thus, the iterative procedure of Figure 6 avoids uncertainties related to the estimation of hull condition from observations on the hull, and also the fact that experimental testing of representative hull roughness geometries would otherwise be required. However, the fact that vessel performance data is required for estimating the hull roughness condition introduces other uncertainties, related to the quality of the logged data (sensor accuracy, sampling, manual input errors, etc.), accuracy of power-speed relations for obtaining the expected shaft power,

and the validity of corrections for relative wind and sea state. At this point, such uncertainties are not quantified, and only a crude comparison to values of hull roughness estimated from divers' reports has been attempted, yielding promising results (Figure 8). Using either of the two procedures, i.e. the original Granville method or the iterative procedure of Figure 6, modelling errors are always introduced, as the hull resistance under smooth/rough conditions is represented by a flat plate model, and shaft power penalties are dependent also on modelling of propeller-hull interactions, i.e. the estimated propulsive coefficient η_D .

4.4. Future work and recommendations

In this section, future work on the above topics is suggested, with clear indication of what will be included in the on-going project. Some final recommendations are given for stakeholders in the field.

Regarding matching of cleaning forces on adhesion strength of marine organisms, the following aspects can be highlighted for future work:

- need for adhesion strength data of microfouling on biocide-containing coatings (included in the project);
- need for adhesion strength values of fouling communities, i.e. complex communities instead of single-species communities (included);
- need for accurate estimation of hydrodynamic forces on experimental setups for testing adhesion strength of microfouling (included);
- determination of medium/long-term effects of grooming tools on biocide-containing coatings, where grooming tools are operated as to remove fouling using minimal forces (included);
- determination of forces imparted by commercial cleaning tools actuating over low-profile roughness surfaces, such as coatings and microfouled surfaces (outside the scope of the project).

Regarding the estimation of hull penalties due to hull roughness, the following aspects can be highlighted for future work, however outside the scope of the current project:

- following a hull-condition-to-penalty approach, further research would be needed for relating roughness measurements on the hull (surface statistics) to hydrodynamic parameters such as the roughness function and equivalent sand roughness height, which would require significant effort not only in terms of experimental testing of different hull conditions, but also in terms of development of practical methods for in-water hull roughness characterization;
- alternatively, if vessel performance data is to be used, the quality and quantity of logged data and external information on the vessel must be further analysed in order to estimate and reduce uncertainties;
- the validity of the form factor approach should be further tested, especially on slow vessels with high form factor, i.e. less slender vessels;
- models for propeller-hull interaction with varying hull roughness should be developed, using self-propulsion numerical studies or sea trial data;
- finally, a full techno-economic analysis of hull biofouling management is required on a case-by-case basis (commercial management), together with global and local guidelines on in-water maintenance to minimize chemical and biological contamination (IMO and national level).

Recommendations for involved stakeholders working in the field of biofouling and in-water hull maintenance are given below:

- for **researchers, standard-developers and other staff working with adhesion strength of macrofouling**, the occurrence of cohesive failure during such tests should be reported, e.g. as a percentage of failed measurements; thus, a high cohesive failure rate might indicate underestimation of the base plate's adhesive strength, as only the loosely attached individuals are pooled (assuming fairly constant mechanical properties for shells of the same sample);
- for **hull cleaning technology developers**, there is a large incentive to develop autonomous or remotely operated solutions, as research indicates it is preferable to target initial stages of fouling using a hull

grooming approach that demands highly frequent intervention; also, it would be valuable to quantify the forces exerted by each cleaning tool, in terms of surface pressure and shear stress, in order to select the optimal settings for a particular cleaning job;

- for **diving companies, ship owners and port/municipality decision makers**, in-water hull cleaning of established macrofouling should be avoided as much as possible; for example, regular grooming during a prolonged idle periods (e.g. during vessel lay-up) is encouraged, as opposed to responsive, heavy-duty cleaning by the end of idle period.
- for **ship technical managers**, speed-independent indicators of hull performance should be preferred, e.g. the hydraulic roughness k_s obtained using the iterative procedure of Figure 6, as opposed to percentage speed loss or percentage power increase. Furthermore, a form factor approach on hull roughness penalties cannot be generalised for all speeds, particularly when more than 12% of the total resistance corresponds to wave making resistance, as this resistance component is also affected by hull roughness (Paper II).

5. Conclusions

Biofouling on underwater ship hulls can contribute to significant fuel penalties, associated with economic, societal and environmental issues. This thesis presents tools for improving current practices related to hull performance management, focusing on the adhesion strength of marine organisms on different coatings (Paper I) and estimation of fouled-hull penalties (Paper II).

In Paper I, knowledge gaps that hinder better matching of cleaning forces to adhesion strength of marine organisms were identified, and conclusions were derived from published adhesion strength data on different substrata. From this adhesion-strength perspective, it is arguably better to invest in combating microfouling rather than macrofouling. Furthermore, suggestions are given for improving current methods of determining adhesion strength, namely the reporting of cohesive failure, i.e. reporting the percentage of discarded measurements due to shell breakage.

Regarding the benefits of hull cleaning from a fuel-saving perspective, Paper II demonstrates that the hull form might be an important parameter at low speeds (less than 12% wave-making resistance) and for less slender vessels, such as tankers. However, the Granville method without form-factor corrections provides fairly accurate results, when compared to CFD simulations. This thesis further applied the Granville method in estimating the hull condition, i.e. the equivalent sand roughness height, from vessel monitored data (noon reports). The estimated sand roughness height can be used as an indicator of the hull condition, with the advantage of being independent from vessel speed, which is not the case for other indicators such as percentage speed loss.

Future research should work towards optimizing other aspects of underwater hull cleaning, such as finding optimal cleaning intervals and forces that do not significantly reduce the effectiveness and lifetime of the paint. Focus should be given to AF coatings, which currently dominate the market and will probably continue to dominate in the near future, especially for relatively slow vessels on which FR coatings are not as effective. Also, it is noted that adhesion strength of complex natural marine microfouling on AF coatings is practically absent from the literature, and this information is required for better designing cleaning devices aiming at minimal forces for microfouling removal.

THE ENEMY BELOW

References

- Ackerman, J. D. et al. (1992) 'Investigation of zebra mussel adhesion strength using rotating disks', *Journal of Environmental Engineering*, (118), pp. 708–724.
- AMBIO (2010) The Publishable Final Activity Report of the AMBIO Integrated Project (Project No. NMP4-CT-2005-011827).
- Anderson, K. and Bows, A. (2012) 'Executing a Scharnow turn: reconciling shipping emissions with international commitments on climate change', *Carbon Management*, 3(6), pp. 615–628.
- ASTM D4939–89 (2003) Standard Test Method for Subjecting Marine Antifouling Coating to Biofouling and Fluid Shear Forces in Natural Seawater (Reapproved 2003), Standard Test Method. West Conshohocken, PA, United States.
- ASTM D5618 (1994) Measurement of Barnacle Adhesion Strength in Shear (Reapproved 2000), Standard Test Method. West Conshohocken, PA, United States.
- Balashov, V. S. et al. (2011) 'Cleaning by means of the HISMAR autonomous robot', *Russian Engineering Research*, 31(6), pp. 589–592.
- Berntsson, K. M. et al. (2000) 'Reduction of barnacle recruitment on micro-textured surfaces: Analysis of effective topographic characteristics and evaluation of skin friction', *Biofouling*, 16(2–4), pp. 245–261.
- Bertram, V. (2017) 'Some Heretic Thoughts on ISO 19030', in 2nd Hull Performance & Insight Conference (HullPIC'17). Ulrichshusen, pp. 4–11.
- BIMCO (2013) Hull fouling clause for time charter parties (updated 16 July 2015), Special Circular No. 3. Available at: <https://www.bimco.org/contracts-and-clauses/bimco-clauses> (Accessed: 8 May 2017).
- Bradshaw, P. (2000) 'A note on "critical roughness height" and "transitional roughness"', *Physics of Fluids*, 12(6), p. 1611.
- Brady, R. F. and Singer, I. L. (2000) 'Mechanical factors favoring release from fouling release coatings', *Biofouling*, 15(1–3), pp. 73–81.
- Briand, J.-F. et al. (2017) 'Spatio-Temporal Variations of Marine Biofilm Communities Colonizing Artificial Substrata Including Antifouling Coatings in Contrasted French Coastal Environments', *Microbial Ecology*. *Microbial Ecology*.
- Brock, R., Bailey-Brock, J. H. and Goody, J. (1999) 'A case study of efficacy of freshwater immersion in controlling introduction of alien marine fouling communities: The USS Missouri', *Pacific Science*, 53(3), pp. 223–231.

- BRS (2017) BRS Group Annual Report 2017. Available at: http://www.brsbrokers.com/review_archives.php.
- Cal, R. B. et al. (2009) 'The rough favourable pressure gradient turbulent boundary layer', *Journal of Fluid Mechanics*, 641, p. 129.
- Callow, J. A. and Callow, M. E. (2006) 'The Ulva Spore Adhesive System', in Smith, A. M. and Callow, J. A. (eds) *Biological Adhesives*. Berlin: Springer-Verlag, pp. 63–78.
- Candries, M. (2000) 'Paint systems for the marine industry', *Paint systems for the marine industry: Notes to Complement the external seminar on Antifoulings*, (December), pp. 1–27.
- Candries, M. et al. (2003) 'The measurement of the drag characteristics of tin-free self-polishing co-polymers and fouling release coatings using a rotor apparatus.', *Biofouling*, 19 Suppl(September 2015), pp. 27–36.
- Candries, M. and Atlar, M. (2005) 'Experimental Investigation of the Turbulent Boundary Layer of Surfaces Coated With Marine Antifoulings', *Journal of Fluids Engineering*, 127(2), p. 219.
- Carlton, J. S. (2007) 'Service performance and analysis', in *Marine Propellers and Propulsion*. 2nd edn. Oxford: Butterworth Heinemann, pp. 477–502.
- Cassé, F. et al. (2007) 'Laboratory screening of coating libraries for algal adhesion.', *Biofouling*, 23(3–4), pp. 267–276.
- Castro, A. M., Carrica, P. M. and Stern, F. (2011) 'Full scale self-propulsion computations using discretized propeller for the KRISO container ship KCS', *Computers and Fluids*. Elsevier Ltd, 51(1), pp. 35–47.
- Cebeci, T. and Bradshaw, P. (1977) *Momentum transfer in boundary layers*. New York: Hemisphere Publishing Corporation / McGraw-Hill Book Company.
- Champ, M. A. (2000) 'A review of organotin regulatory strategies, pending actions, related costs and benefits', *Science of the Total Environment*, 258(1–2), pp. 21–71.
- Chiovitti, A., Dugdale, T. M. and Wetherbee, R. (2006) 'Diatom Adhesives: Molecular and Mechanical Properties', in Smith, A. M. and Callow, J. A. (eds) *Biological Adhesives*. Berlin: Springer-Verlag, pp. 79–103.
- Corbett, J. J., Winebrake, J. J. and Lauer, A. (2007) 'Mortality from Ship Emissions: A Global Assessment', *Environmental Science & Technology*, 41(24), pp. 8512–8518.
- Coutts, A. D. M., Taylor, M. D. and Hewitt, C. L. (2007) 'Novel method for assessing the en route survivorship of biofouling organisms on various vessel types', *Marine Pollution Bulletin*, 54(1), pp. 97–100.
- Crisp, D. . et al. (1985) 'Adhesion and substrate choice in mussels and barnacles',

- Journal of Colloid and Interface Science, 104(1), pp. 40–50.
- Davidson, I. C. et al. (2009) 'The role of containerships as transfer mechanisms of marine biofouling species.', *Biofouling*, 25(7), pp. 645–655.
- Demirel, Y. K., Turan, O. and Incecik, A. (2017) 'Predicting the effect of biofouling on ship resistance using CFD', *Applied Ocean Research*. Elsevier B.V., 62, pp. 100–118.
- Drake, J. M. and Lodge, D. M. (2007) 'Hull fouling is a risk factor for intercontinental species exchange in aquatic ecosystems', *Aquatic Invasions*, 2(2), pp. 121–131.
- Dürr, S. and Thomason, J. C. (2009a) *Biofouling*, *Biofouling*. Edited by S. Drr and J. C. Thomason. Oxford, UK: Wiley-Blackwell.
- Dürr, S. and Thomason, J. C. (2009b) *Biofouling*, *Biofouling*. Edited by S. Drr and J. C. Thomason. Oxford, UK: Wiley-Blackwell.
- Earley, P. J. et al. (2014) 'Life cycle contributions of copper from vessel painting and maintenance activities', *Biofouling*, 30(1), pp. 51–68.
- Finlay, J. A. et al. (2002) 'Adhesion Strength of Settled Spores of the Green Alga *Enteromorpha*', *Biofouling*, 18(4), pp. 251–256.
- Flack, K. A. and Schultz, M. P. (2010) 'Review of Hydraulic Roughness Scales in the Fully Rough Regime', *Journal of Fluids Engineering*, 132(4), p. 41203.
- Flack, K. A. and Schultz, M. P. (2014) 'Roughness effects on wall-bounded turbulent flows', *Physics of Fluids*, 26(10), p. 101305.
- Freire-González, J. and Puig-Ventosa, I. (2015) 'Energy efficiency policies and the Jevons paradox', *International Journal of Energy Economics and Policy*, 5(1), pp. 69–79.
- Gangadharan, S. N. et al. (2001) 'Experimental investigation of *Enteromorpha clathrata* biofouling on lifting surfaces of marine vehicles', *Marine Technology*, 38(1), pp. 31–50.
- Grigson, C. (1987) 'Full-scale viscous drag of actual ship surfaces and the effect of quality of roughness on predicted power', *Journal of Ship Research*, 31(3), pp. 189–206.
- Haslbeck, E. G. and Bohlander, G. (1992) 'Microbial Biofilm Effects on Drag -Lab and Field', *Proceedings of the Ship Production Symposium*.
- Hearin, J. et al. (2015) 'Analysis of long-term mechanical grooming on large-scale test panels coated with an antifouling and a fouling-release coating', *Biofouling*, 31(8), pp. 625–638.
- Hearin, J. et al. (2016) 'Analysis of mechanical grooming at various frequencies

- on a large scale test panel coated with a fouling-release coating', *Biofouling*, 32(5), pp. 561–569.
- Holm, E. R. et al. (2004) 'Evaluation of hydrodynamic drag on experimental fouling-release surfaces, using rotating disks.', *Biofouling*, 20(4–5), pp. 219–226.
- Holm, E. R., Haslbeck, E. G. and Horinek, A. a (2003) 'Evaluation of brushes for removal of fouling from fouling-release surfaces, using a hydraulic cleaning device.', *Biofouling*, 19(5), pp. 297–305.
- Hunsucker, J. T. et al. (2016) 'Influence of hydrodynamic stress on the frictional drag of biofouling communities', *Biofouling*. Taylor & Francis, 32(10), pp. 1209–1221.
- Hutchins, N. et al. (2016) 'Turbulent boundary layers developing over rough surfaces: from the laboratory to full-scale systems', in 20th Australasian Fluid Mechanics Conference - December 2016. Perth (AUS).
- IMO (2001) International Convention On the Control of Harmful Anti-Fouling Systems on Ships. London: The Stationery Office Limited.
- IMO (2011a) 'Guidelines for the control and management of ships' biofouling to minimize the transfer of invasive aquatic species', in Resolution MEPC.207(62), pp. 1–25.
- IMO (2011b) MEPC 63/4/8: A transparent and reliable hull and propeller performance standard.
- IMO (2014) Reduction of GHG emissions from ships - Third IMO GHG Study 2014 - Final Report, MEPC 67/INF.3. Available at: [http://www.imo.org/en/OurWork/Environment/PollutionPrevention/AirPollution/Documents/Third Greenhouse Gas Study/GHG3 Executive Summary and Report.pdf](http://www.imo.org/en/OurWork/Environment/PollutionPrevention/AirPollution/Documents/Third%20Greenhouse%20Gas%20Study/GHG3%20Executive%20Summary%20and%20Report.pdf) (Accessed: 1 June 2017).
- ISO (2016) ISO 19030:2016 - Ships and marine technology - Measurement of changes in hull and propeller performance, ISO/TC 8/SC 2. Available at: http://www.iso.org/iso/home/store/catalogue_tc/catalogue_detail.htm?number=63774 (Accessed: 1 June 2017).
- ITTC (2011) The 1978 ITTC Performance Prediction Method, 26th International Towing Tank Conference. Rio de Janeiro: ITTC. Available at: <http://ittc.info/downloads/proceedings/> (Accessed: 1 June 2017).
- Johansson, L.-E. (1984) 'The local effect of hull roughness on skin friction', *RINA Transactions*, 127, pp. 187–201.
- Johnson, H. and Andersson, K. (2014) 'Barriers to energy efficiency in shipping', *WMU Journal of Maritime Affairs*.
- Kamino, K. (2006) 'Barnacle Underwater Attachment', in Smith, A. M. and Callow, J. A. (eds) *Biological Adhesives*. Berlin: Springer-Verlag, pp. 145–166.

- Larsson, A. I., Granhag, L. and Jonsson, P. R. (2016) 'Instantaneous flow structures and opportunities for larval settlement: barnacle larvae swim to settle', *PLoS ONE*, 11(7), p. e0158957.
- Larsson, L. and Raven, H. C. (2010a) Decomposition of Resistance. In: *The Principles of Naval Architecture Series - Ship Resistance and Flow*. Jersey City (NJ): The Society of Naval Architects and Marine Engineers.
- Larsson, L. and Raven, H. C. (2010b) 'Governing Equations', in *The Principles of Naval Architecture Series - Ship Resistance and Flow*, pp. 5–9.
- Larsson, L. and Raven, H. C. (2010c) 'Similarity', in *The Principles of Naval Architecture Series - Ship Resistance and Flow*, pp. 10–13.
- Larsson, L. and Raven, H. C. (2010d) The Flow Around the Hull and the Viscous Resistance. In: *The Principles of Naval Architecture Series - Ship Resistance and Flow*. Edited by J. R. Paulling. Jersey City (NJ): The Society of Naval Architects and Marine Engineers.
- Lee, J. H. (2015) 'Turbulent boundary layer flow with a step change from smooth to rough surface', *International Journal of Heat and Fluid Flow*. Elsevier Inc., 54, pp. 39–54.
- Leer-Andersen, M. and Larsson, L. (2003) 'An experimental/numerical approach for evaluating skin friction on full-scale ships with surface roughness', *Journal of marine science and technology*, 8, pp. 26–36.
- Lewkowicz, A. K. and Das, D. K. (1986) 'Turbulent boundary layers on rough surfaces with and without a pliable overlayer: a simulation of marine fouling', *International Shipbuilding Progress*, 33(386), pp. 174–186.
- Lewthwaite, J. C., Molland, A. F. and Thomas, K. W. (1984) 'An investigation into the variation of ship skin frictional resistance with fouling', *RINA Transactions*, 127, pp. 269–284.
- Lindholdt, A., Dam-Johansen, K., Olsen, S. M., et al. (2015) 'Effects of biofouling development on drag forces of hull coatings for ocean-going ships: a review', *Journal of Coatings Technology and Research*, 12(3), pp. 415–444.
- Lindholdt, A., Dam-Johansen, K., Yebra, D. M., et al. (2015) 'Estimation of long-term drag performance of fouling control coatings using an ocean-placed raft with multiple dynamic rotors', *Journal of Coatings Technology Research*, 12(6), pp. 975–995.
- Lindner, E. (1988) 'Failure mechanism of copper antifouling coatings', *International Biodeterioration*, 24(4–5), pp. 247–253.
- Malone, J. A. (1980) 'Effects of Hull Foulants and Cleaning/Coating Practices on Ship Performances and Economics', *Transactions - Society of Naval Architects and Marine Engineers*, 88, pp. 75–101.

- Meng, Q., Du, Y. and Wang, Y. (2016) 'Shipping log data based container ship fuel efficiency modeling', *Transportation Research Part B: Methodological*. Elsevier Ltd, 83, pp. 207–229.
- Molland, A. F. (2008) 'Chapter 10 - Underwater vehicles', in *The Maritime Engineering Reference Book*, pp. 728–783.
- Monty, J. P. et al. (2016) 'An assessment of the ship drag penalty arising from light calcareous tubeworm fouling', *Biofouling*, 32(4), pp. 451–464.
- Morrisey, D. et al. (2013) *In-water cleaning of vessels : Biosecurity and chemical contamination risks*. Wellington, New Zealand: Ministry of Primary Industries.
- Morrisey, D. and Woods, C. M. C. (2015) *In-water cleaning technologies: Review of information Prepared for Ministry for Primary Industries*. Available at: <http://www.mpi.govt.nz/news-and-resources/publications/> (Accessed: 30 Oct 2017).
- Moser, C. S. et al. (2016) 'Quantifying the total wetted surface area of the world fleet: a first step in determining the potential extent of ships??? biofouling', *Biological Invasions*. Springer International Publishing, 18(1), pp. 265–277.
- Munk, T., Kane, D. and Yebra, D. M. (2009) *The effects of corrosion and fouling on the performance of ocean-going vessels: a naval architectural perspective*. In: *Advances in marine antifouling coatings and technologies*. Oxford (UK): Woodhead Publishing Limited.
- Nasdaq (2017) *End of day commodity futures price quotes for crude oil WTI (NYMEX)*. Available at: <http://www.nasdaq.com/> (Accessed: 3 May 2017).
- Nikuradse, J. (1933) *Strömungsgesetze in rauhen Röhren [Laws of Flow in Rough Pipes]*. Forschungsheft 361 [translated as National Advisory Committee for Aeronautics, 1950, Technical Memorandum 1292]. Göttingen (DE): Verein Deutscher Ingenieure - Verlag.
- NSTM (2006) *Chapter 081 – Water-borne underwater hull cleaning of Navy ships*. Washington DC.
- Nygren, C. (2002) 'TBT-Free Antifouling Paints: One Company's Experience', *JPCL-PMC*, (January), pp. 44–50.
- Pedersen, B. P. (2015) *Data-driven Vessel Performance Monitoring of Ships*. DTU.
- Perry, A. E. and Li, J. D. (1990) 'Experimental support for the attached-eddy hypothesis in zero-pressure-gradient turbulent boundary layers', *Journal of Fluid Mechanics*, 218, p. 405.
- Pettitt, M. E. et al. (2004) 'Activity of commercial enzymes on settlement and adhesion of cypris larvae of the barnacle *Balanus amphitrite*, spores of the green alga *Ulva linza*, and the diatom *Navicula perminuta*.', *Biofouling*, 20(6), pp. 299–311.

- Plutarch (no date) 'Symposiacs', in Hamm, J. et al. (eds) *Essays and Miscellanies*. 5th (2013). London: Project Gutenberg. Available at: www.gutenberg.org.
- Pu, X., Li, G. and Huang, H. (2016) 'Preparation, anti-biofouling and drag-reduction properties of a biomimetic shark skin surface', *Biology Open*, 0, pp. 1–8.
- Railkin, A. I. (2004) *Marine Biofouling - Colonization Processes and Defenses / by Alexander I. Railkin; translators, Tatiana A. Ganf and Oleg G. Manylov*. CRC Press LLC.
- Raven, H. C. et al. (2008) 'Towards a CFD-based prediction of ship performance - progress in predicting full-scale resistance and scale effects', *Transactions of the Royal Institution of Naval Architects Part A: International Journal of Maritime Engineering*, 150(4), pp. 31–42.
- Rehmatulla, N. and Smith, T. (2015) 'Barriers to energy efficiency in shipping: A triangulated approach to investigate the principal agent problem', *Energy Policy*, 84, pp. 44–57.
- Ricketts, J. B. and Hundley, L. L. (1997) 'Naval Ship Self-Assessment of Hull Powering Performance Using Propulsion Shaft Torsionmeters and GPS', *Naval Engineers Journal*, (May), pp. 181–192.
- Rittschof, D. et al. (2008) 'Barnacle reattachment: a tool for studying barnacle adhesion', *Biofouling*, 24(1), pp. 1–9.
- Rompay, B. Van (2013) 'Is the Much Sought-After, Better Alternative Underwater Hull Coating System Already Here?', *Marine Coatings*, (April).
- Sagert, J., Sun, C. and Waite, J. (2006) 'Chemical subtleties of mussel and polychaete holdfasts', in Smith, A. M. and Callow, J. A. (eds) *Biological Adhesives*. Berlin: Springer-Verlag, pp. 125–143.
- Schlichting, H. (1979) *Boundary-layer theory*. Kestin J, translator. 7th Ed. Edited by J. R. Holman. New York (NY): McGraw-Hill, Inc.
- Schottle, R. and Brown, P. (2007) 'Copper loading assessment from in-water hull cleaning following natural fouling, Shelter Island Yacht Basin, San Diego Bay, San Diego, California', *Ports 2007*, pp. 1–10.
- Schultz, M. P. et al. (2000) 'A turbulent channel flow apparatus for the determination of the adhesion strength of microfouling organisms', *Biofouling*, 15(4), pp. 243–251.
- Schultz, M. P. (2000) 'Turbulent Boundary Layers on Surfaces Covered With Filamentous Algae', *Journal of Fluids Engineering*, 122(2), p. 357.
- Schultz, M. P. et al. (2003) 'Three models to relate detachment of low form fouling at laboratory and ship scale', *Biofouling*, 19 Suppl(September 2015), pp. 17–

26.

Schultz, M. P. (2004) 'Frictional Resistance of Antifouling Coating Systems', *Journal of Fluids Engineering*, 126(6), p. 1039.

Schultz, M. P. (2007) 'Effects of coating roughness and biofouling on ship resistance and powering', *Biofouling*, 23(5–6), pp. 331–341.

Schultz, M. P. et al. (2011) 'Economic impact of biofouling on a naval surface ship', *Biofouling*, 27(1), pp. 87–98.

Schultz, M. P. et al. (2015) 'Impact of diatomaceous biofilms on the frictional drag of fouling-release coatings', *Biofouling*, 31(9–10), pp. 759–773.

Schultz, M. P. and Swain, G. W. (1999) 'The Effect of Biofilms on Turbulent Boundary Layers', *Journal of Fluids Engineering*, 121(1), p. 44.

Stacey, A. and Stacey, J. (2012) 'Integrating Sustainable Development into Research Ethics Protocols Centre for Sustainability in Mining and Industry, University of the', *Electronic Journal of Business Research Methods*, 10(2), pp. 54–63.

Stopford, M. (2009) *Maritime Economics*. 3rd edn. Oxford (UK): Routledge.

Subramanian, C. S., Shinjo, N. and Gangadharan, S. N. (2004) 'A study of hydrodynamic characteristics of boundary layer with algae roughness', *Marine Technology and Sname News*, 41(2), pp. 60–66.

Svensen, T. (1983) 'A techno-economic model of ship operation with special reference to hull and propeller maintenance in the face of uncertainty', II (March).

Swain, G. (1999) 'Redefining Antifouling Coatings', *JPCL-PMC*, (9), pp. 26–35.

Swain, G. and Shinjo, N. (2014) 'Comparing Biofouling Control Treatments for Use on Aquaculture Nets', pp. 22142–22154.

Swain, G. W., Nelson, W. G. and Preedeekanit, S. (1998) 'The influence of biofouling adhesion and biotic disturbance on the development of fouling communities on non-toxic surfaces', *Biofouling*, 12(July 2013), pp. 257–269.

Swain, G. W. and Schultz, M. P. (1996) 'The testing and evaluation of non-toxic antifouling coatings', *Biofouling*, 10(1–3), pp. 187–197.

Takata, L., Falkner, M. and Gilmore, S. (2006) *Commercial Vessel Fouling in California: analysis, evaluation, and recommendations to reduce nonindigenous species release from the non-ballast water vector*, California State Lands Commission, April 2006.

Thomas, K. V and Brooks, S. (2010) 'The environmental fate and effects of antifouling paint biocides.', *Biofouling*, 26(1), pp. 73–88.

- Townsin, R. (1991) 'The correlation of added drag with surface roughness parameters', *Recent Developments in Turbulence Management*, pp. 181–191.
- Townsin, R. L. et al. (1980) 'Speed, power and roughness: the economics of outer bottom maintenance', *Naval Architect*, (2), pp. 459–483.
- Townsin, R. L. (2003) 'The ship hull fouling penalty', *Biofouling*, 19, pp. 9–15.
- Townsin, R. L. and Anderson, C. D. (2009) 'Fouling control coatings using low surface energy, foul release technology', *Advances in Marine Antifouling Coatings and Technologies*, pp. 693–708.
- Tribou, M. and Swain, G. W. (2010) 'The use of proactive in-water grooming to improve the performance of ship hull antifouling coatings.', *Biofouling*, 26(1), pp. 47–56.
- Tribou, M. and Swain, G. W. (2015) 'Grooming using rotating brushes as a proactive method to control ship hull fouling', *Biofouling*, 31(4), pp. 309–319.
- UNCTAD (2016) *Review of Maritime Transport 2016*.
- Watermann, B. et al. (1997) 'Performance and effectiveness of non-stick coatings in seawater', *Biofouling*, 11(2), pp. 101–118.
- Wood, C. D. et al. (2000) 'Temporal and spatial variations in macrofouling of silicone fouling-release coatings', *Biofouling*, 16(2–4), pp. 311–322.
- Woods Hole Oceanographic Institute (1952) *Marine fouling and its prevention*. Menasha, WI: George Banta Publishing Co.
- Yebra, D. M., Kiil, S. and Dam-Johansen, K. (2004) 'Antifouling technology - Past, present and future steps towards efficient and environmentally friendly antifouling coatings', *Progress in Organic Coatings*, 50(2), pp. 75–104.
- Yeginbayeva, I. et al. (2016) 'Investigating the Impact of Surface Condition on the Frictional Resistance of Fouling Control Coating Technologies', in *31st Symposium on Naval Hydrodynamics - September 2016*. Monterey (CA).
- Ünal, U. O., Ünal, B. and Atlar, M. (2012) 'Turbulent boundary layer measurements over flat surfaces coated by nanostructured marine antifouling', 52, pp. 1431–1448.

Paper I

Review

Matching Forces Applied in Underwater Hull Cleaning with Adhesion Strength of Marine Organisms

Dinis Oliveira * and Lena Granhag

Department of Shipping and Marine Technology, Chalmers University of Technology,
SE 412 96 Gothenburg, Sweden; lena.granhag@chalmers.se

* Correspondence: dinis@chalmers.se; Tel.: +46-31-772-6701

Academic Editors: Christine Bressy, Jean-François Briand, Gérald Culioli and André Margaillan

Received: 30 August 2016; Accepted: 7 October 2016; Published: 17 October 2016

Abstract: Biofouling is detrimental to the hydrodynamic performance of ships. In spite of advances in hull coating technology, a ship must usually undergo underwater hull cleaning to remove biofouling during her in-service time. However, some cleaning practices may also lead to decreased lifetime of the fouling-control coating. Therefore, cleaning forces should be minimized, according to the adhesion strength of marine organisms present on the hull. In this article, values of adhesion strength found in available literature are discussed in the light of current knowledge on hull cleaning technology. Finally, the following knowledge gaps are identified: (1) data on adhesion strength of naturally-occurring biofouling communities are practically absent; (2) shear forces imparted by current cleaning devices on low-form fouling (microfouling) and corresponding effects on hull coatings are largely unknown. This knowledge would be valuable for both developers and users of cleaning technology.

Keywords: biofouling; barnacle; adhesion strength; microfouling; macrofouling; ship hull cleaning; ship hull grooming

1. Introduction

Biofouling, the colonization of a surface by living organisms (Figure 1), is detrimental to the hydrodynamic performance of ships, through increased roughness of the hull and propeller, meaning higher fuel consumption or lower maximum speed [1]. Furthermore, it is associated with biosecurity concerns, as a mean of transport of non-native invasive species (NIS) [2]. Importantly, coating systems used for reducing or preventing biofouling are associated with high application and maintenance costs, and may cause water pollution through the release of toxic substances [1].

Increased roughness on the ship hull and propeller contributes to increased hull frictional resistance and decreased propeller efficiency, respectively, both translating into increased power consumption, or decreased speed [3]. It is estimated that a thin slime, “just detectable by touch” (microfouling), can lead to an increase in local skin friction of 25% compared to a clean hull [4]. Schultz et al. further compared the condition of a heavily slimed hull to that of a newly-painted hull and estimated an increase of ~9% in the fuel consumption for the US Navy’s Arleigh Burke-class destroyer [5]. In broader terms, 9%–12% of global emissions of Greenhouse Gases (GHG) from shipping can be attributed to deterioration of hull and propeller performance, due to both mechanical damage and biofouling [6].

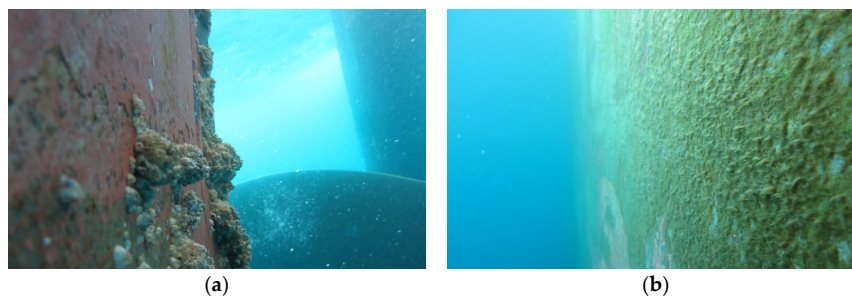


Figure 1. Biofouling on a ship hull—in spite of fouling-control coatings, underwater hull cleaning is still required: (a) hard macrofouling at the stern, consisting of mostly barnacles; (b) soft algal fouling and microfouling on the ship’s side. Photographs courtesy of Marininvest Shipping AB (Gothenburg, Sweden; reproduced with permission).

As a measure against biofouling, use of fouling-control coatings on the underwater hull can lead to significant operational gains (e.g., [7,8]). Recent estimates suggest that, if each vessel was to shift to its respective “best available” paint technology, the world fleet would benefit from an overall 7%–10% savings in fuel, with a corresponding decrease in air emissions [6]. The two main types of fouling-control coatings correspond to Anti-Fouling (AF) coatings—which rely on biocides for preventing settlement of marine organisms—and Foul-Release (FR) coatings—which rely on surface and bulk mechanical properties to decrease adhesion strength [1]. However, to reduce the impact on non-target marine organisms, the release of toxic substances into the environment should be minimized, at every step from paint application to hull blasting [9–11].

In spite of available fouling-control coatings, ships are still required to undergo underwater cleaning to remove biofouling [12], especially when it comes to algal fouling and microfouling (Figure 1b). Since dry docks have limited availability and dry-docking time represents a loss of revenue for commercial ship operators, underwater cleaning is performed during the typical five-year period between dry-dockings [13]. However, if the underwater cleaning is too aggressive, the fouling-control coating can be damaged, with negative consequences to its effectiveness and lifetime [14]. It is therefore important to know, on one side, the adhesion strength of marine organisms, and, on the other side, the forces imparted by cleaning tools, in order to match cleaning forces to the type and intensity of fouling.

This short review article aims at (1) giving an overview of current underwater cleaning technology; (2) analysing previously published adhesion strength values for different groups of marine organisms on different hull coatings and (3) identifying areas for future research on forces and frequency of underwater cleaning. The current focus is on minimizing cleaning forces for low impact on the fouling-control hull paint, i.e., without affecting its long-term efficacy, and also minimizing the release of toxic substances into the marine environment [11,15]. Other important topics related to underwater hull cleaning, such as the risk of inadvertent release of viable organisms and propagules to the marine environment, are reviewed elsewhere [16].

2. Underwater Hull Cleaning and Hull Grooming

As mentioned above, keeping a ship hull relatively clean between dry-dockings sometimes means resorting to underwater cleaning, typically using aggressive methods such as abrasive pads and brushes. As an alternative to cleaning, “hull grooming” has been suggested, defined as a proactive, frequent and more gentle mechanical maintenance of the hull [5,17]. Except for special cases, in which abrasive conditioning of the coating is desirable (e.g., the so-called “surface treated composites” [18]), forces used during underwater cleaning event should remain as low as possible, in order to maximize the lifetime of the coating [19].

Most common technologies for removing biofouling rely on brushes or water jets [20,21]. Alternative methods that aim at preventing/killing biofouling without removing it are also in

use, like for example heat treatment and encapsulation. However, while encapsulation is probably more adequate for recreational vessels and still requires standardisation [22,23], the efficacy of heat treatments on large areas of the hull is still lacking independent evaluation and no recent publications could be found since the last available review from 2010 [20].

Forces imparted by brush systems have been studied for specific types of brushes and reported shear forces are in order of 10 kPa [14,24]. However, these results correspond to specific barnacle geometries (instrumented studs are used, representing barnacles), and no data are yet available on actual forces imparted on other forms of fouling, i.e., macrofoulers other than barnacles, and microfouling. Information on the latter is of particular relevance, considering that proposed brush grooming tools are unable to remove tenacious biofilms (low-form, strongly adhered biofilms) that form under frequent grooming [25]. These biofilms can still have a significant impact on hull hydrodynamic performance, depending on intensity and coverage [26].

It is recognized that brush-systems can erode, or even damage, fouling-control coatings [20,24]. However, reporting on the effects of brushes on hull coatings (e.g., scratching and wear) is limited to a few cleaning devices [14,15,25,27]. In addition, imparted forces are dependent on several factors, such as the type of surface used for cleaning (i.e., carpet, scouring pad or brush), geometrical parameters (for brushes: bristle density, angle and stiffness), standoff distance and wearing of the cleaning surface, e.g., at the tip of bristles in cleaning brushes [24,28]. Comparatively easier to estimate, forces imparted by water jets on the coating are dependent on impact pressure, nozzle diameter and standoff distance [29]. However, the maximum shear force at the wall will still be dependent on the actual roughness of the surface to be cleaned [30], thus varying with surface geometry of the coating/biofouling. To the best of our knowledge, there are currently no studies on forces imparted by water jets on fouled or coated surfaces.

Finally, the above comments apply to easily accessible and relatively flat surfaces of the hull. However, variability in cleaning forces might arise across the hull surface, depending on the cleaning method and the existence of “niche areas” (appendages and sheltered areas), where cleaning devices need to be tailored.

3. Adhesion Strength of Marine Organisms

Adhesion strength can be defined as the force required for removing a marine organism from a given surface, expressed as force per unit area ($\text{N}/\text{m}^2 = \text{Pa}$). Knowledge of such values is valuable not only for comparing the efficacy of different FR coatings, where low adhesion is targeted, but also as a reference for selecting minimal forces for underwater hull cleaning/grooming [14].

In this section, which is divided into macro- and microfouling, adhesion strength values available in the literature are reviewed, together with an overview of adhesion and failure mechanisms. Emphasis is given here on macroscopic methods of measuring adhesive strength, since we aim at directly translating these results into shear forces necessary for cleaning. Still, microscopic methods are also available, such as Atomic Force Microscopy (AFM), enabling topographical and mechanical characterization of cells and adhesives, for both macrofoulers [31] and microfoulers [32].

3.1. Macrofouling

Barnacles are the most comprehensively studied group of macrofoulers. However, several other relevant groups of macrofoulers must be considered, such as mussels, oysters, tubeworms (polychaetes) and macroalgae. Each group of organisms is associated with its particular adhesion mechanism. Thus, for instance, whereas barnacles, oysters, tubeworms and macroalgae adhere permanently to a surface in their adult stage, adult mussels are still able to move by breaking the byssus threads that keep them anchored to a given location and by growing new threads [33].

Barnacles have different phases of adhesion: temporary adhesion occurs firstly, as the cypris larva explores a surface; secondly, the larva produces a settlement cement; finally, the metamorphosed adult barnacle produces a stronger cement, leading to permanent settlement [33,34]. Adhesion strength is

For relatively high adhesion strength (e.g., for epoxy coatings), it is not uncommon for cohesive failure to occur, which means that the shell of the organism is broken and measurements do not represent adhesion strength: thus, the force necessary to produce adhesive failure, i.e., complete removal of the shell, is larger than that required for breaking the shell. In the event of cohesive failure, a fraction of the shell remains attached to the surface. Different criteria have been used for dealing with such occurrence: in earlier studies, readings were corrected for the fraction of base plate detached [50,51]; Berglin et al. suggested to quantitatively use the transition from cohesive to adhesive failure as a performance indicator for FR coatings [36]; finally, as standard procedure in ASTM Standard D5618-94, readings are usually considered void if more than 10% of the organism's adhered surface remains on the coating [35]. However, using the latter standard procedure, even if readings with extensive cohesive failure are considered void, the occurrence of cohesive failure may indicate that the actual adhesion strength for that population is underestimated, since cohesive strength sets an upper bound to the measurable adhesion strength. However, very few authors report the rejection percentage (e.g., [47,48]), important information that could indicate underestimation of adhesion strength. Additionally, cohesive failure is a challenge for underwater cleaning, since remaining baseplates contribute to hull/propeller roughness, while possibly decreasing the long-term effectiveness of the fouling-control paint, as discussed below in Section 4.

Finally, values of adhesion strength for oysters and tubeworms on silicone FR coatings are also given at the lower part of Figure 2. These do not seem to differ significantly from those of barnacles, although more data would be needed for a fair comparison. While adhesion mechanisms of barnacles and mussels are well studied, those of oysters and tubeworms have not received so much attention [52]. Again, the incidence of cohesive failure is unknown for available studies on the adhesion strength of oysters and tubeworms.

3.2. Microfouling

The groups of microfoulers that receive most attention in terms of adhesion strength include marine bacteria, benthic diatoms (microalgae) and spores/sporelings of macroalgae. Although the latter spores (i.e., propagules) and sporelings (i.e., young plants) correspond to early development stages of a macroalgae, they are usually considered as microfouling, due to size.

Bacteria and benthic diatoms rely on building up a layer of insoluble Extracellular Polymeric Substances (EPS) in order to adhere to a surface, constituting a biofilm. EPS is mostly composed of carbohydrates [53], but proteins might also play an important role in adhesion, and treatment with proteases has been observed to reduce the adhesion strength of diatom *Navicula perminuta* [54]. After settlement, many benthic diatom species are reported to "glide" on the surface once adhesion takes place, leaving behind a trail of adhesive [53].

Adhesion mechanisms of early stages of macroalgae differ markedly from those of bacterial and diatom biofilms. *Ulva* is the most commonly occurring macroalgae on ship hulls [55]. It produces motile spores (zoospores) that swim by means of flagella and are capable of selective settlement. Thus, once the right environmental and surface cues are offered, a spore will permanently attach by means of secreted adhesive [56].

Values of adhesion strength for different microfouling species and stages of development are given in Figure 3 for more than 80% removal, and Figures 4 and 5 for more than 50% removal and for diatoms and early stages of macroalgae, respectively. All the values correspond to silicone FR coatings.

Due to the reduced size of these organisms, hydrodynamic methods are routinely employed for measuring adhesion strength, replacing the mechanical shear test presented above for macrofoulers [56]. These hydrodynamic methods include the turbulent flow apparatus [57], calibrated water jet apparatus [29] and automated water jet apparatus [58]. The use of different methods may also contribute to some of the variability in the presented data.

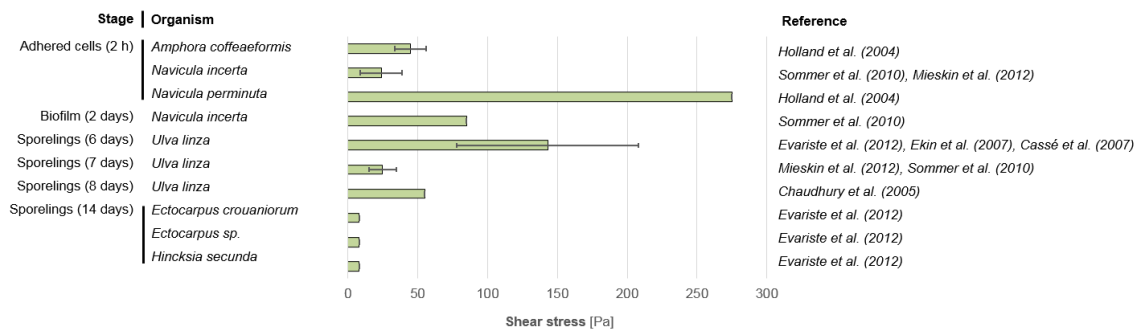


Figure 3. Adhesion strength values for microfoulers (diatoms and early stages of development of macroalgae) on different formulations of silicone Foul-Release (FR) coatings (full data in Supplementary Materials), given as shear stress required for >80% removal. Error bars correspond to the uncertainty estimated by individual studies (when available) or, where more than one study is cited, to standard deviation between different studies. For studies using water jet systems [45,55,59,60], originally reported jet impact pressures were converted to maximum shear stress using the same formula as in [29]. Cited articles: Holland et al. [59], Sommer et al. [45], Mieskin et al. [61], Evariste et al. [62], Ekin et al. [55], Cassé et al. [58], and Chaudhury et al. [63].

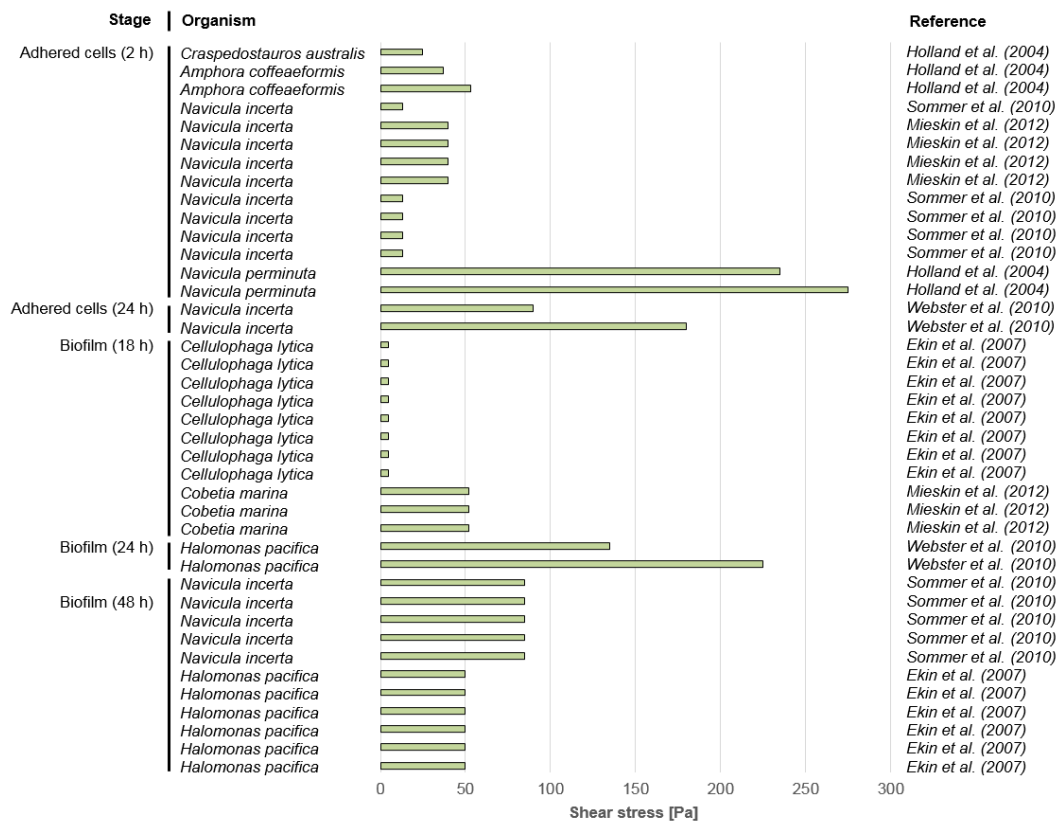


Figure 4. Adhesion strength values for diatoms on different formulations of silicone Foul-Release (FR) coatings (full data in Supplementary Materials), given as shear stress required for >50% removal. For studies using water jet systems [45,55,59,60], originally reported jet impact pressures were converted to maximum shear stress using the same formula as in [29]. Cited articles: Holland et al. [59], Sommer et al. [45], Mieskin et al. [61], Webster et al. [48] and Ekin et al. [55].

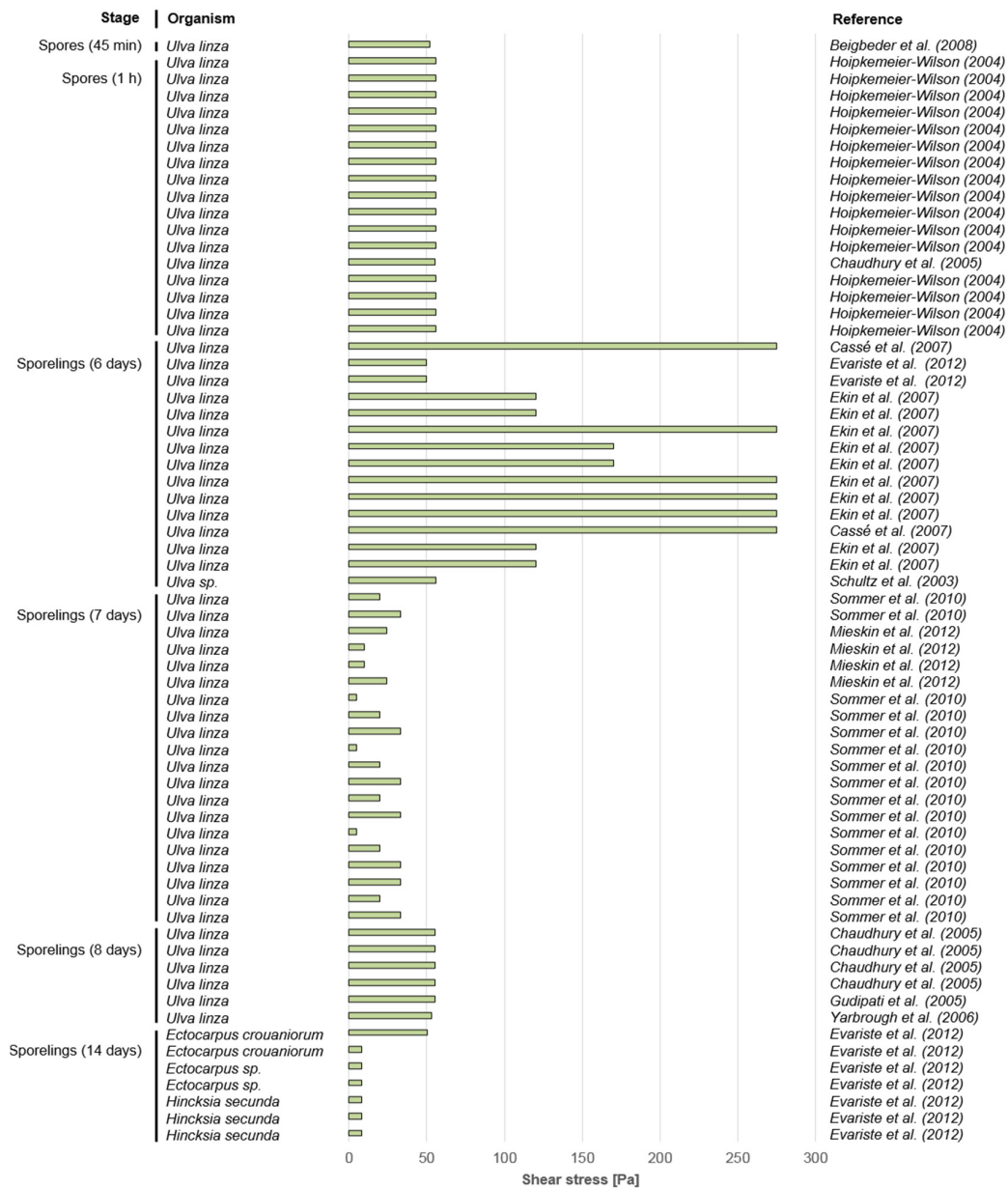


Figure 5. Adhesion strength values for macroalgae (early stages of development) on different formulations of silicone FR coatings (full data in Supplementary Materials), given as shear stress required for >50% removal. For studies using water jet systems [45,55,59,60], originally reported jet impact pressures were converted to maximum shear stress using the same formula as in [29]. Cited articles: Beigbeder et al. [64], Hoipkemeier-Wilson [65], Chaudhury et al. [63], Cassé et al. [58], Evariste et al. [62], Ekin et al. [55], Schultz et al. [66], Sommer et al. [45], Mieszkin et al. [61], Gudipati et al. [67] and Yarborough et al. [68].

Adhesion strength is given as an applied shear stress, which must be taken together with the corresponding percentage removal and treatment time (usually 5 min for the turbulent flow apparatus [57]). This creates an issue when comparing results from different studies, since at least two values are considered, i.e., the shear stress and percentage removal. As a criterion, shear stress values presented in Figure 3 have been selected for >80% removal, meaning that an initially 100%-fouled surface would have been cleaned by at least 80%. Here, we assume that removal is independent from the initial percentage cover, although it is possible that percentage cover affects removal, considering that it is known to affect wall shear forces [26].

From Figure 3, adhered diatom cells (*Amphora coffeaeformis*, *Navicula incerta* and *Navicula perminuta*), in contact with the surface for 2 h, could be removed by applying shear stresses of ~20 to 275 Pa, whereas a two-day-old biofilm of *Navicula incerta* would require an intermediate shear stress. Sporelings of macroalgae (Figure 3: *Ulva linza*, *Ectocarpus crouaniorum*, *Ectocarpus* sp. and *Hinckesia secunda*) are usually tested after growing for six to 14 days, and their adhesion strength on silicone FR coatings varies from ~8 Pa to ~140 Pa. Overall, Figure 3 provides reference values of adhesion strength valuable for deciding on minimum cleaning forces for silicon FR coatings. However, it should be stressed that variability is introduced by differences in surface properties of each FR coating tested within each study (see Supplementary Materials).

Values of adhesion strength corresponding to >50% removal are presented in Figures 4 and 5, for diatoms and early stages of macroalgae, respectively. Here, the minimum reported value corresponds to 5 Pa, for both 18-h-old biofilm of *Cellulophaga lytica* and seven-day-old sporelings of *Ulva linza*. For *Navicula incerta* (Figure 4), adhesion strength is apparently higher when a biofilm is allowed to form, as compared to isolated adhered cells. For macroalgae (Figure 5), it is noted that adhesion strength reaches its maximum values at around one week. As the algae grows, there is usually an increase in reported removal from FR coatings [66]. This is probably due to an increase in the length of the algae filaments (increased protrusion leads to increased drag) rather than lower adhesive properties of older sporelings, at least on FR coatings. This might not be true for all surfaces, since such positive relation between percentage removal and age could not be found on glass [66].

From the above results, at least two species stand out as having higher adhesion strength: these are *Navicula perminuta* and *Ulva linza*. The later is a widely spread macroalgae [56]. Differences between species can be partially attributed to the use of different hydrodynamic methods, for e.g., in Holland et al. [59], but at least one study (Evariste et al.) seems to indicate superior adhesion strength of *Ulva linza*, compared to other macroalgae species [62]. Besides the already mentioned variability in surface properties of different FR coatings, it is not entirely clear, from the literature, to what extent large differences between species (up to one order of magnitude) can be attributed to intrinsic properties of adhesives produced by different species [59] or to different exposure to hydrodynamic stress due to different geometry of cells/sporelings [66].

As noted before for macrofoulers, values of adhesion strength on coatings other than FR are largely missing in the literature. This is possibly due to the focus on the efficacy of FR coatings, rather than forces necessary for cleaning coatings currently in use on the majority of ship hulls. The number of species studied is also limited, whereas results obtained from single species are likely to differ from those obtained using natural communities (multi-species samples). On the latter aspect, a first step has been taken by Mieszkin et al., who studied variations in adhesion strength of *Ulva linza* and *Navicula incerta* on differently pre-conditioned coated surfaces (natural biofilm and *Cobetia marina* biofilm) [61]. Results from the latter study indicate complex relationships between algae and marine biofilms, suggesting that over-generalization should be avoided.

4. Matching Cleaning/Grooming Forces with Adhesion Strength

Thus far, we have discussed how cleaning/grooming is performed and how its forces are measured/estimated (Section 2). Furthermore, we reviewed published results of adhesion strength of marine organisms (Section 3). The remaining question is how well these forces can be matched.

For macrofouling, adhesion strength values of Figure 2 can be directly compared to cleaning forces measured on instrumented studs [14,24]. Thus, for example, the grooming tool suggested by Tribou et al. imparts a shear stress of approx. 0.01 MPa [14], and it would thus be unable to remove an average macrofouler from even a silicone FR coating, since the minimum value in Figure 2 corresponds to 0.03 MPa. However, it can still be effective against minimally adhered macrofoulers [14]. On the other hand, too high a cleaning shear stress means an increased risk of damaging the AF/FR coating, whereas, as pointed out by Bohlander, the amount of paint removal depends also on paint type and age [21]. For an ablative AF paint, Hearin et al. report an area extent of wear

(or erosion) of $12\% \pm 10\%$ of the topcoat after 12-month grooming on a weekly/bi-weekly basis (shear stress ~ 0.01 MPa), whereas ungroomed control surfaces suffered significantly higher wear, with a $31\% \pm 20\%$ removal of the topcoat. This difference was attributed to higher forces used in hand-cleaning the ungroomed control surfaces prior to the photographic visual inspection. For an FR coating, Hearin et al. found no wear of the topcoat, but only localised damage, which was attributed to causes other than the grooming itself [27]. In addition, the coating system adheres to the hull with finite strength, which poses an upper limit to forces that can be used during cleaning. Although adhesion of the coating to the hull varies significantly with application quality and exposure conditions [69], the strength of ship hull coatings is normally 2.5–3 MPa [70], which is comparable to adhesion strength values mentioned above for macrofouling on epoxy coatings. Besides wear/damage to the AF/FR coating system, high cleaning shear stress will also increase the frequency of cohesive failure, i.e., shell breakage (Section 3.1), which means an imperfect result from the cleaning, thus contributing to the frictional drag of the vessel. Cohesive failure may also bring about negative consequences for the subsequent long-term effectiveness of the paint, since shell remains could intensify later recruitment by providing chemical cues for settlement [71]. All these factors support the use of hull grooming, targeting early stages of fouling.

Unfortunately, it is not possible to compare adhesion strength values of microfouling (Figures 3–5) to cleaning forces measured on instrumented studs, since imparted forces strongly depend on the geometry of the surface to be cleaned. Although there are data on instrumented barnacles (e.g., [14]), to the best of our knowledge, data are not yet available on shear forces imparted by any brush/pad system on either microfouled surfaces or coated surfaces. Thus, in addition to estimations of shear forces for water jet systems on rough surfaces [30], a collection of values of shear stress from different types of brushes/pads as a function of fouling roughness would enable valid comparisons to be drawn. In turn, this would enable matching cleaning/grooming forces with adhesion strength of microfouling, which is considered the best target for a more coating-friendly underwater hull maintenance.

From the above, recommendations can be summarized as follows, for different stakeholders working with underwater hull cleaning:

- for developers of cleaning technology: (1) shear forces should target microfouling or early stages of macrofouling; (2) forces should be easy to control by the user, with as few adjustable parameters as possible; (3) variability in shear force for each level of cleaning strength should be minimized; and (4) information should be compiled on effects on different types of coatings, microfouled samples and surface roughness;
- for users (e.g., diving companies), ship owners and as tool for various decision makers: (1) underwater cleaning of hulls covered with macrofouling should be avoided, as a rule; (2) the cleaning strength level should be adjusted by taking into account information available from the manufacturer of the cleaning system, as to get a conservatively low first estimate of strength needed for the task, taking into consideration the type and age of coating.

5. Conclusions

In this short review, we discussed the issue of matching forces used in hull cleaning/grooming to the actual fouling condition of the hull, consisting of a multi-species combination of macro- and microfouling. It is apparent that more data will be necessary in order to accomplish this objective. On the one hand, data on adhesion strength of naturally occurring biofouling communities are needed; particularly, data are lacking for adhesion strength of biofouling occurring on AF coatings (biocide-containing coatings). On the other hand, better knowledge is needed on the shear forces imparted by current cleaning devices on low-form fouling (i.e., microfouling), as well as their effects on today's fouling-control coatings. This information would be relevant in designing improved cleaning tools, as practical guidance for divers and ship owners, and as support for decision makers at environmental agencies.

Supplementary Materials: The following are available online at <http://www.mdpi.com/2077-1312/4/4/66/s1>, Spreadsheet S1: Values of Adhesion Strength from Available Literature.

Acknowledgments: The authors would like to express their appreciation for helpful and encouraging comments received from anonymous reviewers. The ongoing project on biofouling is funded by the Swedish Energy Agency (grant agreement 2014-004848). The costs for publishing in Open Access were covered by Chalmers Library, via Chalmers Fund for Open Access 2016. The authors would also like to acknowledge a travel grant awarded to a poster presentation of the present work at the 18th International Congress on Marine Corrosion and Fouling (ICMCF 2016), granted by the US Navy Office of Naval Research (ONR Award N62909-16-1-2026).

Author Contributions: Dinis Oliveira collected the data on adhesion strength from available literature (Spreadsheet S1); Dinis Oliveira and Lena Granhag wrote the paper.

Conflicts of Interest: The authors declare no conflict of interest. The founding sponsors had no role in the design of the study; in the collection, analyses, or interpretation of data, in the writing of the manuscript, and in the decision to publish the results.

References

1. Dürr, S.; Thomason, J.C. *Biofouling*; Dürr, S., Thomason, J.C., Eds.; Wiley-Blackwell: Oxford, UK, 2009.
2. Drake, J.M.; Lodge, D.M. Hull fouling is a risk factor for intercontinental species exchange in aquatic ecosystems. *Aquat. Invasions* **2007**, *2*, 121–131. [[CrossRef](#)]
3. Townsin, R.L. The Ship Hull Fouling Penalty. *Biofouling* **2003**, *19*, 9–15. [[CrossRef](#)] [[PubMed](#)]
4. Lewthwaite, J.C.; Molland, A.F.; Thomas, K.W. An Investigation into the Variation of Ship Skin Frictional Resistance with Fouling. In *RINA Transactions*; The National Academies of Sciences, Engineering, and Medicine: Washington, DC, USA, 1984; pp. 269–284.
5. Schultz, M.P.; Bendick, J.A.; Holm, E.R.; Hertel, W.M. Economic Impact of Biofouling on a Naval Surface Ship. *Biofouling* **2011**, *27*, 87–98. [[CrossRef](#)] [[PubMed](#)]
6. International Maritime Organization (IMO). *A Transparent and Reliable Hull and Propeller Performance Standard*; MEPC 63/4/8; IMO: London, UK, 2011; pp. 1–6.
7. Blanco-Davis, E.; del Castillo, F.; Zhou, P. Fouling Release Coating Application as an Environmentally Efficient Retrofit: A Case Study of a Ferry-Type Ship. *Int. J. Life Cycle Assess.* **2014**, *19*, 1705–1715. [[CrossRef](#)]
8. Champ, M.A. A Review of Organotin Regulatory Strategies, Pending Actions, Related Costs and Benefits. *Sci. Total Environ.* **2000**, *258*, 21–71. [[CrossRef](#)]
9. Schulz, S.; Pastuch, J. How One Shipyard Is Making Paint Removal Cleaner and Greener. *JPLC* **2003**, *20*, 50–54.
10. Song, Y.C.; Woo, J.H.; Park, S.H.; Kim, I.S. A Study on the Treatment of Antifouling Paint Waste from Shipyard. *Mar. Pollut. Bull.* **2005**, *51*, 1048–1053. [[CrossRef](#)] [[PubMed](#)]
11. Earley, P.J.; Swope, B.L.; Barbeau, K.; Bundy, R.; McDonald, J.; Rivera-Duarte, I. Life Cycle Contributions of Copper from Vessel Painting and Maintenance Activities. *Biofouling* **2014**, *30*, 51–68. [[CrossRef](#)] [[PubMed](#)]
12. International Maritime Organization (IMO). *2011 Guidelines for the Control and Management of Ships' Biofouling to Minimize the Transfer of Invasive Aquatic Species*; MEPC 62/24/Add.1; IMO: London, UK, 2011; pp. 1–25.
13. Takata, L.; Falkner, M.; Gilmore, S. *Commercial Vessel Fouling in California: Analysis, Evaluation, and Recommendations to Reduce Nonindigenous Species Release from the Non-Ballast Water Vector*; California State Lands Commission, Marine Facilities Division: Sacramento, CA, USA, 2006.
14. Tribou, M.; Swain, G.W. Grooming Using Rotating Brushes as a Proactive Method to Control Ship Hull Fouling. *Biofouling* **2015**, *31*, 309–319. [[CrossRef](#)] [[PubMed](#)]
15. Schottle, R.; Brown, P. Copper Loading Assessment from in-Water Hull Cleaning Following Natural Fouling, Shelter Island Yacht Basin, San Diego Bay, San Diego, California. In Proceedings of the 11th Triennial International Conference on Ports, San Diego, CA, USA, 25–28 March 2007; pp. 1–10.
16. Floerl, O.; Norton, N.; Inglis, G.J.; Hayden, B.; Middleton, C.; Smith, M.; Alcock, N.; Fitridge, I. *Efficacy of Hull Cleaning Operations in Containing Biological Material—I. Risk Assessment*; MAF Biosecurity: Wellington, New Zealand, 2005.
17. Tribou, M.; Swain, G.W. The Use of Proactive in-Water Grooming to Improve the Performance of Ship Hull Antifouling Coatings. *Biofouling* **2010**, *26*, 47–56. [[CrossRef](#)] [[PubMed](#)]

18. Van Rompay, B. Is the Much Sought-After, Better Alternative Underwater Hull Coating System Already Here? In Proceedings of the RINA, Royal Institution of Naval Architects—International Conference on Marine Coatings, London, UK, 18 April 2013; pp. 38–43.
19. NSTM. *Chapter 081—Water-Borne Underwater Hull Cleaning of Navy Ships*; Direction Of Commander, Naval Sea Systems Command: Washington, DC, USA, 2006.
20. Floerl, O.; Peacock, L.; Seaward, K.; Inglis, G. *Review of Biosecurity and Contaminant Risks Associated with in-Water Cleaning*; Commonwealth of Australia: Canberra, Australia, 2010.
21. Bohlander, J. *Review of Options for in-Water Cleaning of Ships*; MAF Biosecurity: Wellington, New Zealand, 2009.
22. Roche, R.C.; Monnington, J.M.; Newstead, R.G.; Sambrook, K.; Griffith, K.; Holt, R.H.F.; Jenkins, S.R. Recreational Vessels as a Vector for Marine Non-Natives: Developing Biosecurity Measures and Managing Risk through an in-Water Encapsulation System. *Hydrobiologia* **2015**, *750*, 187–199. [[CrossRef](#)]
23. Atalah, J.; Brook, R.; Cahill, P.; Fletcher, L.M.; Hopkins, G.A. It's a Wrap: Encapsulation as a Management Tool for Marine Biofouling. *Biofouling* **2016**, *32*, 277–286. [[CrossRef](#)] [[PubMed](#)]
24. Holm, E.R.; Haslbeck, E.G.; Horinek, A. Evaluation of Brushes for Removal of Fouling from Fouling-Release Surfaces, Using a Hydraulic Cleaning Device. *Biofouling* **2003**, *19*, 297–305. [[CrossRef](#)] [[PubMed](#)]
25. Hearin, J.; Hunsucker, K.Z.; Swain, G.; Gardner, H.; Stephens, A.; Lieberman, K. Analysis of Mechanical Grooming at Various Frequencies on a Large Scale Test Panel Coated with a Fouling-Release Coating. *Biofouling* **2016**, *32*, 561–569. [[CrossRef](#)] [[PubMed](#)]
26. Schultz, M.P.; Walker, J.M.; Steppe, C.N.; Flack, K.A. Impact of Diatomaceous Biofilms on the Frictional Drag of Fouling-Release Coatings. *Biofouling* **2015**, *31*, 759–773. [[CrossRef](#)] [[PubMed](#)]
27. Hearin, J.; Hunsucker, K.Z.; Swain, G.; Stephens, A.; Gardner, H.; Lieberman, K.; Harper, M. Analysis of Long-Term Mechanical Grooming on Large-Scale Test Panels Coated with an Antifouling and a Fouling-Release Coating. *Biofouling* **2015**, *31*, 625–638. [[CrossRef](#)] [[PubMed](#)]
28. Useche, L.V.V.; Wahab, M.M.A.; Parker, G.A. Brush Dynamics: Models and Characteristics. In Proceedings of the ASME 8th Biennial Conference on Engineering Systems Design and Analysis, Volume 3: Dynamic Systems and Controls, Symposium on Design and Analysis of Advanced Structures, and Tribology, Torino, Italy, 4–7 July 2006; pp. 441–450.
29. Finlay, J.A.; Callow, M.; Schultz, M.P.; Swain, G.W.; Callow, J.A. Adhesion Strength of Settled Spores of the Green Alga *Enteromorpha*. *Biofouling* **2002**, *18*, 251–256. [[CrossRef](#)]
30. Rajaratnam, N.; Mazurek, K.A. Impingement of Circular Turbulent Jets on Rough Boundaries. *J. Hydraul. Res.* **2005**, *43*, 689–695. [[CrossRef](#)]
31. Guo, S.; Khoo, B.C.; Teo, S.L.M.; Zhong, S.; Lim, C.T.; Lee, H.P. Effect of ultrasound on cyprid footprint and juvenile barnacle adhesion on a fouling release material. *Colloid Surface B* **2014**, *115*, 118–124. [[CrossRef](#)] [[PubMed](#)]
32. Callow, J.A.; Crawford, S.A.; Higgins, M.J.; Mulvaney, P.; Wetherbee, R. The application of atomic force microscopy to topographical studies and force measurements on the secreted adhesive of the green alga *Enteromorpha*. *Planta* **2000**, *211*, 641–647. [[CrossRef](#)] [[PubMed](#)]
33. Crisp, D.J.; Walker, G.; Young, G.A.; Yule, A.B. Adhesion and substrate choice in mussels and barnacles. *J. Colloid Interface Sci.* **1985**, *104*, 40–50. [[CrossRef](#)]
34. Kamino, K. Barnacle Underwater Attachment. In *Biological Adhesives*; Smith, A.M., Callow, J.A., Eds.; Springer: Berlin, Germany, 2006; pp. 145–166.
35. ASTM International. *Measurement of Barnacle Adhesion Strength in Shear (Reapproved 2000)*; ASTM Standard D5618; ASTM International: West Conshohocken, PA, USA, 1994.
36. Berglin, M.; Larsson, A.; Jonsson, P.R.; Gatenholm, P. The adhesion of the barnacle *Balanus improvisus*, to poly(dimethylsiloxane) fouling-release coatings and poly(methyl methacrylate) panels: The effect of barnacle size on strength and failure mode. *J. Adhes. Sci. Technol.* **2001**, *15*, 1485–1502. [[CrossRef](#)]
37. Larsson, A.I.; Mattsson-Thorngren, L.; Granhag, L.M.; Berglin, M. Fouling-Release of Barnacles from a Boat Hull with Comparison to Laboratory Data of Attachment Strength. *J. Exp. Mar. Biol. Ecol.* **2010**, *392*, 107–114. [[CrossRef](#)]
38. Ackerman, J.D.; Ethier, C.R.; Allen, D.G.; Spelt, J.K. Investigation of Zebra Mussel Adhesion Strength Using Rotating Disks. *J. Environ. Eng.* **1992**, *118*, 708–724. [[CrossRef](#)]
39. Swain, G.W.; Nelson, W.G.; Preedeekanit, S. The Influence of Biofouling Adhesion and Biotic Disturbance on the Development of Fouling Communities on Non-toxic Surfaces. *Biofouling* **1998**, *12*, 257–269. [[CrossRef](#)]

40. Zargiel, K.; Swain, G.W. Static vs. Dynamic Settlement and Adhesion of Diatoms to Ship Hull Coatings. *Biofouling* **2014**, *30*, 115–129. [[CrossRef](#)] [[PubMed](#)]
41. Cassé, F.; Swain, G.W. The Development of Microfouling on Four Commercial Antifouling Coatings under Static and Dynamic Immersion. *Int. Biodeterior. Biodegrad.* **2006**, *57*, 179–185. [[CrossRef](#)]
42. Swain, G.W.; Schultz, M.P. The Testing and Evaluation of Non-Toxic Antifouling Coatings. *Biofouling* **1996**, *10*, 187–197. [[CrossRef](#)] [[PubMed](#)]
43. Swain, G.; Anil, A.C.; Baier, R.E.; Chia, F.; Conte, E.; Cook, A.; Hadfield, M.; Haslbeck, E.; Holm, E.; Kavanagh, C.; et al. Biofouling and Barnacle Adhesion Data for Fouling-release Coatings Subjected to Static Immersion at Seven Marine Sites. *Biofouling* **2000**, *16*, 331–344. [[CrossRef](#)]
44. Wood, C.D.; Truby, K.; Stein, J.; Wiebe, D.; Holm, E.; Wendt, D.; Smith, C.; Kavanagh, C.; Montemarano, J.; Swain, G.; Meyer, A. Temporal and Spatial Variations in Macrofouling of Silicone Fouling-Release Coatings. *Biofouling* **2000**, *16*, 311–322. [[CrossRef](#)]
45. Sommer, S.; Ekin, A.; Webster, D.C.; Stafslie, S.J.; Daniels, J.; VanderWal, L.J.; Thompson, S.E.M.; Callow, M.E.; Callow, J.A. A Preliminary Study on the Properties and Fouling-Release Performance of Siloxane-Polyurethane Coatings Prepared from Poly(dimethylsiloxane) (PDMS) Macromers. *Biofouling* **2010**, *26*, 961–972. [[CrossRef](#)] [[PubMed](#)]
46. Majumdar, P.; Stafslie, S.; Daniels, J.; Webster, D.C. High Throughput Combinatorial Characterization of Thermosetting Siloxane-urethane Coatings Having Spontaneously Formed Microtopographical Surfaces. *J. Coat. Technol. Res.* **2007**, *4*, 131–138. [[CrossRef](#)]
47. Chen, Z.; Chisholm, B.; Kim, J.; Stafslie, S.; Wagner, R.; Patel, S.; Daniels, J.; Vander Wal, L.; Li, J.; Ward, K.; et al. UV-Curable, Oxetane-Toughened Epoxy-Siloxane Coatings for Marine Fouling-Release Coating Applications. *Polym. Int.* **2008**, *57*, 879–886. [[CrossRef](#)]
48. Webster, D.C.; Pieper, R.J.; Nasrullah, M.J. Zwitterionic/Amphiphilic Pentablock Copolymers and Coatings Therefrom. U.S. Patent WO 2010/042804 A2, 15 April 2010.
49. Wang, Y.; Betts, D.E.; Finlay, J.A.; Brewer, L.; Callow, M.E.; Callow, J.A.; Wendt, D.E.; Desimone, J.M. Photocurable Amphiphilic Perfluoropolyether/poly(ethylene Glycol) Networks for Fouling-Release Coatings. *Macromolecules* **2011**, *44*, 878–885. [[CrossRef](#)]
50. Becka, A.; Loeb, G. Ease of Removal of Barnacles from Various Polymeric Materials. *Biotechnol. Bioeng.* **1984**, *26*, 1245–1251. [[CrossRef](#)] [[PubMed](#)]
51. Becker, K. Attachment Strength and Colonization Patterns of Two Macrofouling Species on Substrata with Different Surface Tension (in Situ Studies). *Mar. Biol.* **1993**, *117*, 301–309. [[CrossRef](#)]
52. Kavanagh, C.J.; Schultz, M.P.; Swain, G.W.; Stein, J.; Truby, K.; Wood, C.D. Variation in Adhesion Strength of *Balanus eburneus*, *Crassostrea virginica* and *Hydroides dianthus* to Fouling-Release Coatings. *Biofouling* **2001**, *17*, 155–167. [[CrossRef](#)]
53. Chiovitti, A.; Dugdale, T.M.; Wetherbee, R. Diatom Adhesives: Molecular and Mechanical Properties. In *Biological Adhesives*; Smith, A.M., Callow, J.A., Eds.; Springer: Berlin, Germany, 2006; pp. 79–103.
54. Pettitt, M.E.; Henry, S.L.; Callow, M.E.; Callow, J.A.; Clare, A.S. Activity of Commercial Enzymes on Settlement and Adhesion of Cypris Larvae of the Barnacle *Balanus amphitrite*, Spores of the Green Alga *Ulva linza*, and the Diatom *Navicula perminuta*. *Biofouling* **2004**, *20*, 299–311. [[CrossRef](#)] [[PubMed](#)]
55. Ekin, A.; Webster, D.C.; Daniels, J.W.; Stafslie, S.J.; Cassé, F.; Callow, J.A.; Callow, M.E. Synthesis, Formulation, and Characterization of Siloxane-Polyurethane Coatings for Underwater Marine Applications Using Combinatorial High-Throughput Experimentation. *J. Coat. Technol. Res.* **2007**, *4*, 435–451. [[CrossRef](#)]
56. Callow, J.A.; Callow, M.E. The *Ulva* Spore Adhesive System. In *Biological Adhesives*; Smith, A.M., Callow, J.A., Eds.; Springer: Berlin, Germany, 2006; pp. 63–78.
57. Schultz, M.P.; Finlay, J.A.; Callow, M.E.; Callow, J.A. A Turbulent Channel Flow Apparatus for the Determination of the Adhesion Strength of Microfouling Organisms. *Biofouling* **2000**, *15*, 243–251. [[CrossRef](#)]
58. Cassé, F.; Ribeiro, E.; Ekin, A.; Webster, D.C.; Callow, J.A.; Callow, M.E. Laboratory Screening of Coating Libraries for Algal Adhesion. *Biofouling* **2007**, *23*, 267–276. [[CrossRef](#)] [[PubMed](#)]
59. Holland, R.; Dugdale, T.M.; Wetherbee, R.; Brennan, A.B.; Finlay, J.A.; Callow, J.A.; Callow, M.E. Adhesion and Motility of Fouling Diatoms on a Silicone Elastomer. *Biofouling* **2004**, *20*, 323–329. [[CrossRef](#)] [[PubMed](#)]

60. Cassé, F.; Stafslie, S.J.; Bahr, J.A.; Daniels, J.; Finlay, J.A.; Callow, J.A.; Callow, M.E. Combinatorial materials research applied to the development of new surface coatings V. Application of a spinning water-jet for the semi-high throughput assessment of the attachment strength of marine fouling algae. *Biofouling* **2007**, *23*, 121–130. [[CrossRef](#)] [[PubMed](#)]
61. Mieszkin, S.; Martin-Tanchereau, P.; Callow, M.E.; Callow, J.A. Effect of Bacterial Biofilms Formed on Fouling-Release Coatings from Natural Seawater and *Cobetia marina*, on the Adhesion of Two Marine Algae. *Biofouling* **2012**, *28*, 953–968. [[CrossRef](#)] [[PubMed](#)]
62. Evariste, E.; Gachon, C.M.M.; Callow, M.E.; Callow, J.A. Development and Characteristics of an Adhesion Bioassay for Ectocarpoid Algae. *Biofouling* **2012**, *28*, 15–27. [[CrossRef](#)] [[PubMed](#)]
63. Chaudhury, M.K.; Finlay, J.A.; Chung, J.Y.; Callow, M.E.; Callow, J.A. The Influence of Elastic Modulus and Thickness on the Release of the Soft-Fouling Green Alga *Ulva linza* (Syn. *Enteromorpha linza*) from Poly(dimethylsiloxane) (PDMS) Model Networks. *Biofouling* **2005**, *21*, 41–48. [[PubMed](#)]
64. Beigbeder, A.; Degee, P.; Conlan, S.L.; Mutton, R.J.; Clare, A.S.; Pettitt, M.E.; Callow, M.E.; Callow, J.A.; Dubois, P. Preparation and Characterisation of Silicone-Based Coatings Filled with Carbon Nanotubes and Natural Sepiolite and Their Application as Marine Fouling-Release Coatings. *Biofouling* **2008**, *24*, 291–302. [[CrossRef](#)] [[PubMed](#)]
65. Hoipkemeier-Wilson, L.; Schumacher, J.F.; Carman, M.L.; Gibson, A.L.; Feinberg, A.W.; Callow, M.E.; Finlay, J.A.; Callow, J.A.; Brennan, A.B. Antifouling Potential of Lubricious, Micro-Engineered, PDMS Elastomers against Zoospores of the Green Fouling Alga *Ulva* (*Enteromorpha*). *Biofouling* **2004**, *20*, 53–63. [[CrossRef](#)] [[PubMed](#)]
66. Schultz, M.P.; Finlay, J.A.; Callow, M.E.; Callow, J.A. Three Models to Relate Detachment of Low Form Fouling at Laboratory and Ship Scale. *Biofouling* **2003**, *19* (Suppl. S1), 17–26. [[CrossRef](#)] [[PubMed](#)]
67. Gudipati, C.S.; Finlay, J.A.; Callow, J.A.; Callow, M.E.; Wooley, K.L. The Antifouling and Fouling-Release Performance of Hyperbranched Fluoropolymer (HBFP)-Poly(ethylene Glycol) (PEG) Composite Coatings Evaluated by Adsorption of Biomacromolecules and the Green Fouling Alga *Ulva*. *Langmuir* **2005**, *21*, 3044–3053. [[CrossRef](#)] [[PubMed](#)]
68. Yarbrough, J.C.; Rolland, J.P.; DeSimone, J.M.; Callow, M.E.; Finlay, J.A.; Callow, J.A. Contact Angle Analysis, Surface Dynamics, and Biofouling Characteristics of Cross-Linkable, Random Perfluoropolyether-Based Graft Terpolymers. *Macromolecules* **2006**, *39*, 2521–2528. [[CrossRef](#)]
69. Woods Hole Oceanographic Institute. *Marine Fouling and Its Prevention*; Chapter 18; George Banta Publishing Co.: Menasha, WI, USA, 1952; p. 313.
70. Balashov, V.S.; Gromov, B.A.; Ermolov, I.L.; Roskilly, A.P. Cleaning by means of the HISMAR autonomous robot. *Russ. Eng. Res.* **2011**, *31*, 589–592. [[CrossRef](#)]
71. Anil, A.C.; Khandeparker, L.; Desai, D.V.; Baragi, L.V.; Gaonkar, C.A. Larval development, sensory mechanisms and physiological adaptations in acorn barnacles with special reference to *Balanus amphitrite*. *J. Exp. Mar. Bio. Ecol.* **2010**, *392*, 89–98. [[CrossRef](#)]



© 2016 by the authors; licensee MDPI, Basel, Switzerland. This article is an open access article distributed under the terms and conditions of the Creative Commons Attribution (CC-BY) license (<http://creativecommons.org/licenses/by/4.0/>).

